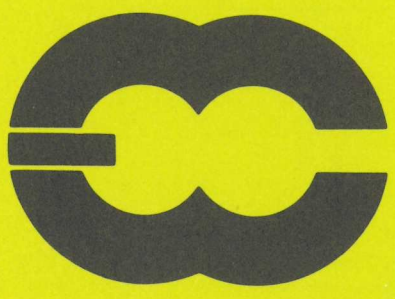

European Centre
for Medium Range
Weather Forecasts

A Routine for Normal Mode Initialization with Non-linear Correction for a Multi-level Spectral Model with Triangular Truncation

Internal Report 15
Research Dept.

August 77.

Centre Européen pour les Prévisions Météorologiques
a Moyen Terme

Europäisches Zentrum Für Mittelfristige Wettervorhersagen

A ROUTINE FOR NORMAL MODE INITIALIZATION WITH NON-LINEAR CORRECTION FOR A MULTI-LEVEL SPECTRAL MODEL WITH TRIANGULAR TRUNCATION

by

Johannes H. Andersen

European Centre for Medium Range Weather Forecasts, Bracknell

Internal Report No. 15

RESEARCH DEPARTMENT

AUGUST 1977

N O T E :

1. Introduction

The idea of performing initialization by combining normal mode analysis with the nonlinear aspects of a numerical model of the atmosphere is due to MACHENHAUER (1977) who has shown that it is possible to determine the gravitational wave part of fields in such a way that the total tendencies of this part of the fields are reduced to a desired epsilon level in a few iterations. The state of zero gravitational wave tendencies cannot in general be fulfilled during an integration, but this imbalance grows only slowly. It was aparently not present in a 24 hour integration with the spectral model at the Institute of Theoretical Meteorology, University of Copenhagen. This model is hemispheric with rhomboidal truncation : M = J = 17, and has 5 vertical levels. The method has the same effect as an ideal dynamic initialization, but operates at a single time level, so the distinction betwen static and dynamic initialization is no longer clear cut. The aim of this report is to give a documentation of the initialization routine,implemented by the author to the global spectral model at ECMWF developed by A.W.HANSEN and A.BAEDE (1977).

2. The model

The formulation of the model is similar to those of BOURKE (1974), HOSKINS and SIMMONS (1975); the choice of vertical levels is optional. The governing prognostic equations of the model are

The vorticity equation :

$$\frac{\partial \xi}{\partial t} = \frac{1}{1-\mu^2}\frac{\partial Jv}{\partial \lambda} - \frac{\partial Ju}{\partial \mu} + F_\xi \qquad (2.1)$$

The divergence equation :

$$\frac{\partial \delta}{\partial t} = \frac{1}{1-\mu^2}\frac{\partial Ju}{\partial \lambda} + \frac{\partial Jv}{\partial \mu} - \nabla^2\left(\frac{U^2 + V^2}{2(1-\mu^2)} + \Phi + \bar{T}\cdot \ln(p_s)\right) + F_\delta \qquad (2.2)$$

The thermodynamic equation :

$$\frac{\partial T'}{\partial t} = -\frac{1}{1-\mu^2}\frac{\partial}{\partial \lambda}(UT') - \frac{\partial}{\partial \mu}(VT') + \delta T' + \gamma\dot{\sigma} - \kappa T(\delta + \frac{\partial \dot{\sigma}}{\partial \sigma}) + F_T \qquad (2.3)$$

The continuity equation :

$$\frac{\partial \ln(p_s)}{\partial t} = -\vec{v}\cdot\nabla\ln(p_s) - \delta - \frac{\partial \dot{\sigma}}{\partial \sigma} \qquad (2.4)$$

The hydrostatic equation :

$$\frac{\partial \Phi}{\partial \ln(\sigma)} = -T \qquad (2.5)$$

From the continuity equation (2.4) with the boundary condition $\dot{\sigma} = 0$ for $\sigma = 0$ and $\sigma = 1$,we get

$$\dot{\sigma} = \int_\sigma^1 (\delta + \vec{v}\cdot\nabla\ln(p_s))d\sigma - (1-\sigma)\int_0^1 (\delta + \vec{v}\cdot\nabla\ln(p_s))d\sigma \qquad (2.6)$$

The meaning of the symbols are

$$Ju = V\cdot(f+\xi) - \dot{\sigma}\frac{\partial U}{\partial \sigma} - T'\frac{\partial \ln(p_s)}{\partial \lambda}$$

$$Jv = -U\cdot(f+\xi) - \dot{\sigma}\frac{\partial V}{\partial \sigma} + T'(\mu^2-1)\frac{\partial \ln(p_s)}{\partial \mu}$$

$\gamma = \kappa\frac{T}{\sigma} - \frac{\partial T}{\partial \sigma}$, the static stability

$U = u \cdot \cos(\phi) = \frac{\partial \chi}{\partial \lambda} + (\mu^2-1)\frac{\partial \psi}{\partial \mu}$

$V = v \cdot \cos(\phi) = -(\mu^2-1)\frac{\partial \chi}{\partial \mu} + \frac{\partial \psi}{\partial \lambda}$

$\xi = \frac{1}{1-\mu^2}\frac{\partial V}{\partial \lambda} - \frac{\partial U}{\partial \mu}$, the relative vorticity

$\delta = \frac{1}{1-\mu^2}\frac{\partial U}{\partial \lambda} + \frac{\partial V}{\partial \mu}$, the divergence

$\vec{v} = u\vec{i} + v\vec{j}$, the velocity vector

$\vec{i}$: unit vector towards east

$\vec{j}$: unit vector towards north

ψ : stream function

χ : velocity potential

ϕ : latitude

λ : longitude

$\mu = \sin(\phi)$

$f = 2\Omega\sin(\phi)$, the coriolis parameter

Ω : angular velocity of earth

$T = \overline{T}(\sigma) + T'$, the temperature

$\overline{T}$: initial horizontal mean temperature

$\kappa = R/c_p$

$\sigma = p/p_s$

p : pressure

p_s: pressure at the surface

R : the gas constant

c_p: specific heat for constant pressure

Φ : the geopotential

Φ_s: surface geopotential (topography)

The F-terms contain contributions from the included physical processes. All fields are non-dimensionalized with radius of earth : a , as unit of length and the reciprocal angular velocity $1/\Omega$ as unit of time. The unit of temperature is $a^2\Omega^2/R$, the geopotential is related to the normalized temperature through the hydrostatic equation (2.5).

3. Linearization

The basic state is chosen as a state at rest and the temperature field equal to $\overline{T}(\sigma)$. The definition of gravity wave fields is determined by the basic state, but for low Rossby numbers, the basic state of zonal mean flow gives almost the same decomposition into gravitational modes, while the frequencies are shifted slightly. MACHENHAUER(1977) found no deterioration by chosing the basic state at rest. The question can be raised where to put the point of separation between linear and non-linear terms, but if this point is chosen in a less complete way, the non-linear correction will compensate the error. This comes also in consideration when physical processes are added to the model.

In order to get a limited eigenvalue-problem, a separation of the numerical equations into vertical and horizontal operations is sought. The variables are considered as column vectors of points on the global sphere containing values of the physical variables in the discrete vertical levels. The notation of HOSKINS and SIMMONS for the vertical operation is adopted in the following. For the purpose we rewrite the model equations.

$$\frac{\partial \xi}{\partial t}\Big| = -\frac{1}{1-\mu^2}\frac{\partial}{\partial \lambda}(fU_{|}) - \frac{\partial}{\partial \mu}(fV_{|}) + Q_{|\xi} \tag{3.1}$$

$$\frac{\partial \delta}{\partial t}\Big| = \frac{1}{1-\mu^2}\frac{\partial}{\partial \lambda}(fV_{|}) - \frac{\partial}{\partial \mu}(fU_{|}) - \nabla^2\left(\Phi_{|} + \overline{T}_{|}\ln(p_s)\right) + Q_{|\delta} \tag{3.2}$$

$$\frac{\partial T}{\partial t}\Big| = -\underline{\underline{\tau}}\delta_{|} + Q_{|T} \tag{3.3}$$

$$\frac{\partial \ln(p_s)}{\partial t} = -\underline{\pi}\delta_{|} + Q_{ps} \tag{3.4}$$

$$\Phi_{|} = \Phi_{s|} + \underline{\underline{G}}T_{|} \tag{3.5}$$

The vertical operators used in these equations

$\underline{\underline{G}}$ is the discrete representation of $\int_{\sigma}^{1}\frac{(\ )}{\sigma}d\sigma$

$\underline{\pi}$ is the discrete representation of $\int_{0}^{1}(\ )d\sigma$

$\underline{\underline{\tau}}$ is the discrete representation of

$$-\frac{\kappa\overline{T}}{\sigma}\int_{0}^{\sigma}(\ )d\sigma + \frac{\partial \overline{T}}{\partial \sigma}\left[\int_{\sigma}^{1}(\ )d\sigma - (1-\sigma)\int_{0}^{1}(\ )d\sigma\right]$$

The Q-terms contain the non-linear contributions to the tendencies. From the equations (3.3)-(3.5) we get

$$\frac{\partial}{\partial t}(\Phi_{|} + \overline{T}_{|}\ln(p_s)) = -\underline{\underline{B}}\delta_{|} + Q_{|\eta} \tag{3.6}$$

where $\underline{\underline{B}} = \underline{\underline{G\tau}} + \overline{T}_{|}\underline{\pi}$ and $Q_{|\eta} = \underline{\underline{G}}Q_{|T} + \overline{T}_{|}Q_{ps}$

The separation of the linear parts of the tendencies is performed by computing the eigenvectors of the matrix $\underline{\underline{B}}$. The eigenvalues will play the role of dimensionless equivalent depths in a series of shallow water models. HOSKINS and SIMMONS have demonstrated that the square roots of the eigenvalues are velocities of horizontal propagation for pure gravity waves with the vertical structure of the eigenvector. In order to be consistent with the work of MACHENHAUER (1977), ELIASEN and MACHENHAUER (1969) we use the following definition for the geopotential

$$\eta_l = \tfrac{1}{2}(\Phi_l + \overline{T}_l \ln(p_s))$$

As the vertical eigenvectors form a complete set, we can expand the fields on the eigenvectors, these being ordered as column-vectors in the matrix $\underline{\underline{W}}$.

$$\eta_l = \underline{\underline{W}}\hat{\eta}_l$$

$$\delta_l = \underline{\underline{W}}\hat{\delta}_l$$

$$\xi_l = \underline{\underline{W}}\hat{\xi}_l$$

The non-linear terms are also expanded, so we get for the vertical mode ℓ :

$$\frac{\partial \hat{\eta}_\ell}{\partial t} = \frac{H_\ell}{2}\,\hat{\delta}_\ell + \hat{Q}_{\ell\eta} \tag{3.7}$$

$$\frac{\partial \hat{\delta}_\ell}{\partial t} = \frac{1}{1-\mu^2}\frac{\partial}{\partial \lambda}(f\hat{V}_\ell) - \frac{\partial}{\partial \mu}(f\hat{U}_\ell) - 2\nabla^2\hat{\eta}_\ell + \hat{Q}_{\ell\delta} \tag{3.8}$$

$$\frac{\partial \hat{\xi}_\ell}{\partial t} = -\frac{1}{1-\mu^2}\frac{\partial}{\partial \lambda}(f\hat{U}_\ell) - \frac{\partial}{\partial \mu}(f\hat{V}_\ell) + \hat{Q}_{\ell\xi} \tag{3.9}$$

Here H_ℓ is the non-dimensional equivalent depth.

The non-linear terms destroy the separation, but in this analysis they are considered as constants. At this step the horizontal dependencies are introduced by a truncated spectral expansion in spherical harmonics. A field; A,is represented by a component vector $A_{m,n}$ or $\underline{A}$ so that A is written as

$$A = \sum_{m=-M}^{M} \sum_{n=|m|}^{M} A_{m,n} P_{m,n}(\mu) e^{im\lambda}$$

the components are obtained by

$$A_{m,n} = \{A\}_{m,n} = \frac{1}{2\pi} \int_0^{2\pi} \int_{-1}^{1} A \, P_{m,n}(\mu) e^{-im\lambda} d\mu d\lambda$$

$P_{m,n}(\mu)$ are normalized associated Legendre functions.

By truncating the expansion of the fields, the linear part of the equation system with spherical harmonic components as variables becomes a finite system. The linear equations separate into zonal wavenumbers m due to the zonal symmetry of the coriolis force. For each zonal wavenumber, the equations are solved by the eigenvalue separation technique. The relation to Hough functions of the solutions is discussed by LONGUET-HIGGINS (1968). With a triangular truncation, the order of the matrix for the system decreases with increasing zonal wavenumber, ending with the order of 2 for the symmetric flow system,which gives only gravitational mode solutions, and a matrix of order 1 for the antisymmetric flow system which gives a Rossby mode solution. Clearly the eigenfunctions of the numerical model at the boundary of the spectral domain are distorted Hough functions, while the eigenvalues have some agreement. For convenience, we drop the reference to the vertical mode ℓ in the following, except for the equivalent depth H_ℓ. Furthermore we put $f = 2\mu$.

$$\tfrac{1}{2}\frac{\partial \eta_{m,n}}{\partial t} = -\frac{H_\ell}{4}\delta_{m,n} \tag{3.10}$$

$$\tfrac{1}{2}\frac{\partial \delta_{m,n}}{\partial t} = \{\mu\xi\}_{m,n} - U_{m,n} - \{\nabla^2\eta\}_{m,n} \tag{3.11}$$

$$\tfrac{1}{2}\frac{\partial \xi_{m,n}}{\partial t} = -\{\mu\delta\}_{m,n} - V_{m,n} \tag{3.12}$$

Some useful spectral relations are

$$\{\mu A\}_{m,n} = D_{m,n}A_{m,n-1} + D_{m,n+1}A_{m,n+1} \tag{3.13}$$

$$\{\nabla^2 A\}_{m,n} = -n(n+1)A_{m,n} \tag{3.14}$$

$$\{(\mu^2-1)\frac{\partial A}{\partial \mu}\}_{m,n} = (n-1)D_{m,n}A_{m,n-1} - (n+2)D_{m,n+1}A_{m,n+1} \tag{3.15}$$

$$\{\frac{\partial A}{\partial \lambda}\}_{m,n} = imA_{m,n} \tag{3.16}$$

where $D_{m,n} = \sqrt{\frac{n^2-m^2}{4n^2-1}}$

We hereby analyse U and V

$$U_{m,n} = (n-1)D_{m,n}\psi_{m,n-1} - (n+2)D_{m,n+1}\psi_{m,n+1} - m(\frac{\chi_{m,n}}{i}) \tag{3.17}$$

$$iV_{m,n} = (n-1)D_{m,n}(\frac{\chi_{m,n-1}}{i}) - (n+2)D_{m,n+1}(\frac{\chi_{m,n+1}}{i}) - m\psi_{m,n} \tag{3.18}$$

From the shifts in n, it is seen that the system (3.10)-(3.12) seperates into two groups: the symmetric flow system with even n-m in (η,δ) and odd n-m in ξ, and the antisymmetric system with reversed parity. The next step is <u>dropping the reference to zonal wavenumber m</u> where not explicitly expressed. A state vector for a given parity can be arranged as follows:

$$x_{|m} = x_{|} = \begin{Bmatrix} \cdot \\ \cdot \\ \cdot \\ \eta_n \\ \tilde{\chi}_n \\ \tilde{\psi}_{n+1} \\ \eta_{n+2} \\ \cdot \\ \cdot \end{Bmatrix}$$

$$\tilde{\chi}_n = \sqrt{\frac{H_\ell}{4}\, n(n+1)}\ \left(\frac{\chi_n}{i}\right)$$

$$\tilde{\psi}_{n+1} = \sqrt{\frac{H_\ell}{4}(n+1)(n+2)}\ \psi_{n+1}$$

So the system (3.10)-(3.12) is written

$$\frac{\partial x}{\partial t}| = 2i\underline{\underline{A}}x_{|}$$

With the transformation ~ we obtain a simple symmetric form of the matrix $\underline{\underline{A}}$ suitable for the numerical eigenvalue-problem.

Band structure of the $\underline{A}$ matrix

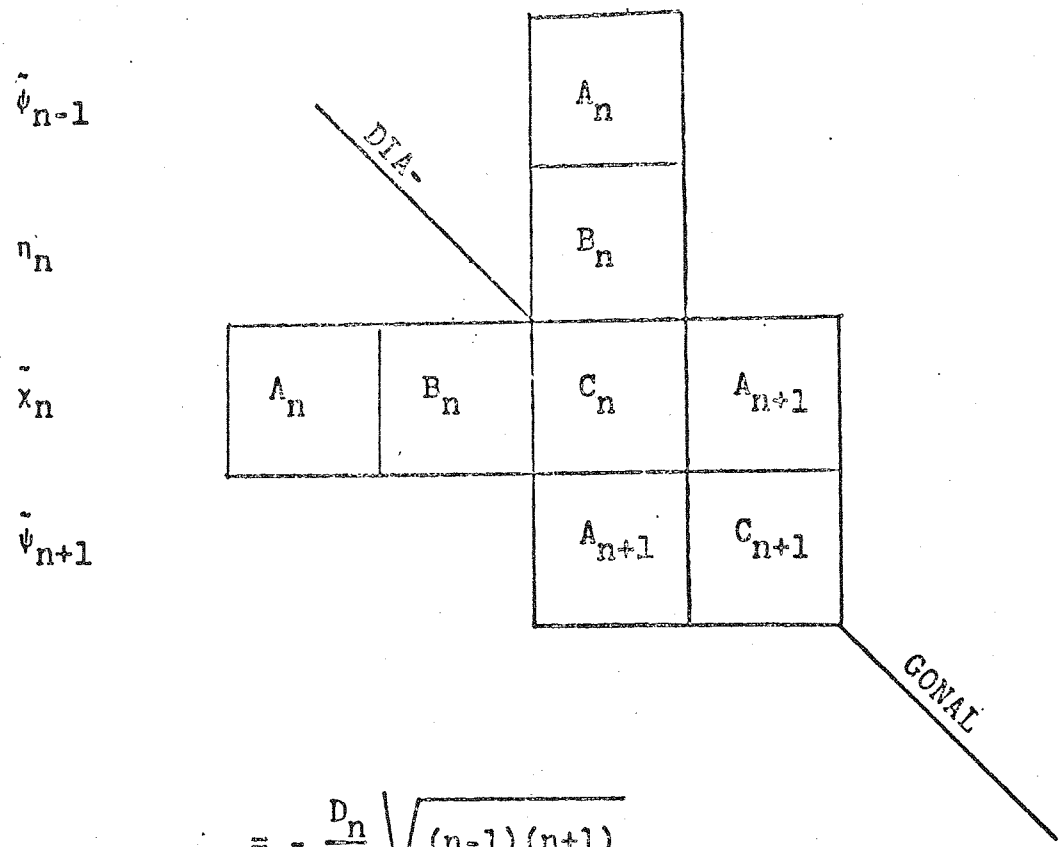

$$\gamma_n = -\frac{D_n}{n}\sqrt{(n-1)(n+1)}$$

$$B_n = \sqrt{\frac{H_e}{4}\, n(n+1)}$$

$$C_n = \frac{m}{n(n+1)}$$

$$D_n = D_{m,n}$$

4. Triangular truncation and matrix order

The maximum meridional number for a field is M-|m|,where M is the triangular truncation limit. This determines the order of the matrix $\underline{\underline{A}}$, and the number of gravity waves: N_{GW} equivalent to the number of divergence and geopotential components in the state vector $x_{|}$. A group consist of 3 components: $(\eta_n, \tilde{\chi}_n, \tilde{\psi}_{n+1})$,symmetric case and $(\tilde{\psi}_n, \eta_{n+1}, \tilde{\chi}_{n+1})$, antisymmetric case. By loading the vector $x_{|}$with these groups (see Fig. 1), N_{GW} is counted up to

$$N_{GW} = \begin{cases} 2((M-|m| + 2)//2) & |m|>0 \quad \text{Sym.} \\ 2((M-|m| + 1)//2) & \text{all m} \quad \text{Antisym.} \end{cases}$$

// means integer division

As the streamfunction components are dominating in the Rossby Waves, we get

$$N_{RW} = \begin{cases} (M - |m| + 1)//2 & \text{all m} \quad \text{Sym.} \\ (M - |m| + 2)//2 & |m|>0 \quad \text{Antisym.} \end{cases}$$

So the order of the matrix adds up to

$$N_{OR} = \begin{cases} 2((M - |m| + 2)//2) + (M - |m| + 1)//2 & \text{Sym.} \\ 2((M - |m| + 1)//2) + (M - |m| + 2)//2 & \text{Antisym.} \end{cases}$$

In Fig.1. an example is demonstrated how N_{OR} depends on meridional limit M-|m| and flow parity.

SYMMETRIC FLOW

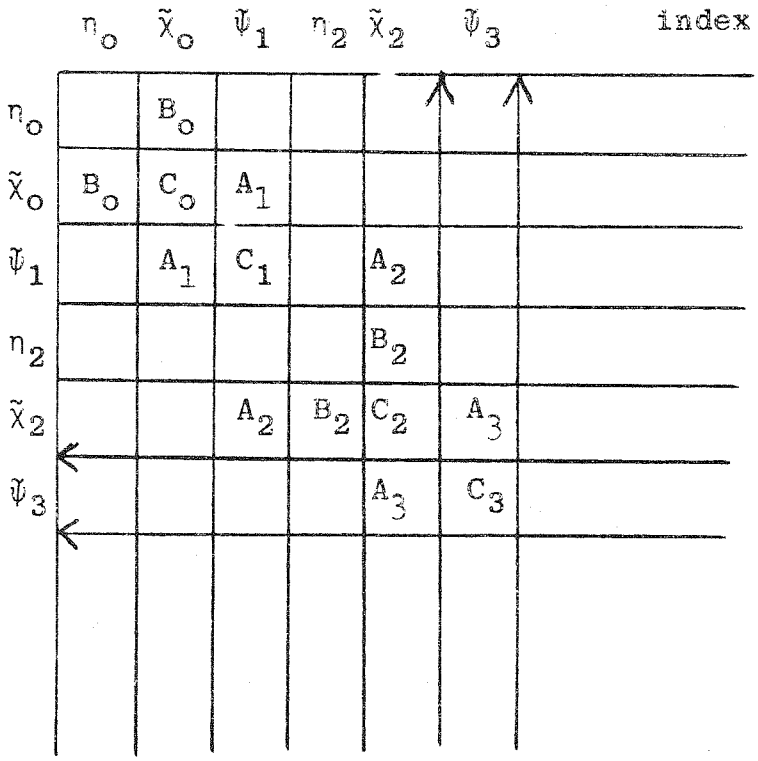

index j = n-m is used

ANTISYMMETRIC FLOW

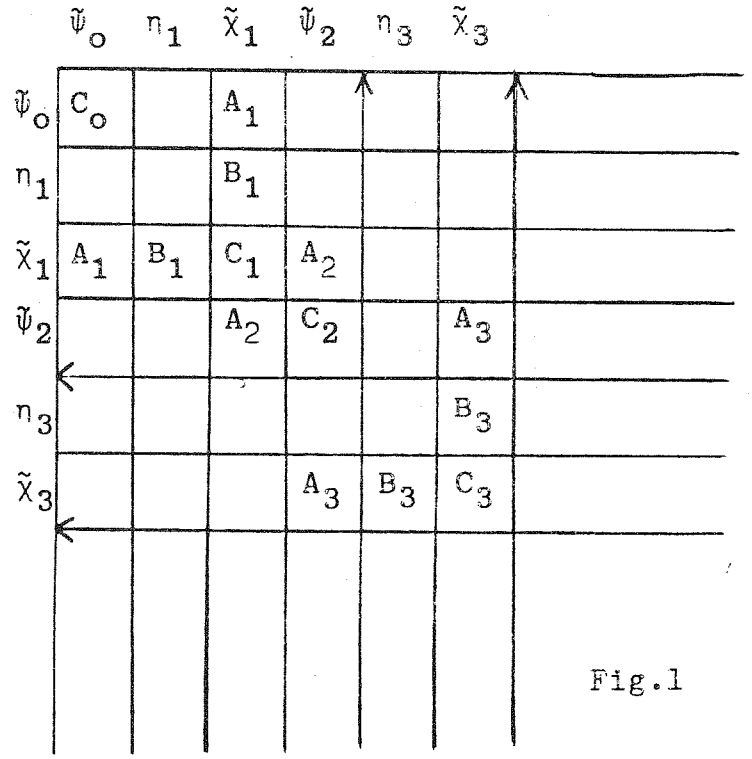

Fig.1

For the zonal fields (m=0) there arises a formal problem of defining $\eta_{o,o}$, $\tilde{\chi}_{o,o}$ and $\tilde{\psi}_{0,0}$. Instead of reducing the matrix, we put 0 in the corresponding matrix elements. The rest of the meaningful components are mapped invariant by the matrix, so the solutions are not changed. We therefore keep the formulae for N_{OR} , but note that N_{GW} is reduced by 2 in the symmetric case, and N_{RW} is reduced by 1 for the antisymmetric case.

$$N_{GW}(0) = 2((M+2)//2) - 2 \qquad \text{Sym.}$$

$$N_{RW}(0) = (M+2)//2 - 1 \qquad \text{Antisym.}$$

All the Rossby wave solutions for m=0 become stationary and degenerate, so the vectors are only conditioned by their spanning of the subspace of zero eigenvalue.

5. An iteration step

The vector $x_|$ is transformed by the orthonormal eigenvectors $\underline{\underline{T}}$ of $\underline{\underline{A}}$ into "Hough-space"

$$y_| = \underline{\underline{T}}^t x_|$$

by which the inhomogeneous system (3.7)-(3.9) becomes

$$\frac{\partial y}{\partial t}| = 2i\underline{\underline{\Lambda}} y_| + \underline{\underline{T}}^t Q_| \qquad (5.1)$$

where $\underline{\underline{\Lambda}} = \underline{\underline{T}}^t \underline{\underline{A}} \underline{\underline{T}}$ is the diagonal matrix of the eigenvalues $q_1 \cdots q_k \cdots$ For a mode k:

$$\frac{\partial y_k}{\partial t} = 2iq_k y_k + r_k$$

The essence of MACHENHAUER's method is to balance out the gravity waves by a search for $\frac{\partial y_k}{\partial t} = 0$, rather than $y_k = 0$. This leads to an iteration scheme for the gravity wave amplitude y_k :

$$y_k^{(n+1)} = - \frac{r_k^{(n)}}{2iq_k} \qquad \text{(the non-linear correction)}$$

or

$$\Delta y_k = y_k^{(n+1)} - y_k^{(n)} = - \frac{1}{2iq_k} \frac{\partial y_k^{(n)}}{\partial t} \tag{5.2}$$

After the correction of y_k, the inverse horizontal and vertical transformations are employed, while the variances of the gravitational and Rossby parts of the fields and tendencies are monitored for each vertical mode.

The problem which is left, is the separation of the correction of η into corrections of geopotential and surface pressure. The gravity waves are filtered out solely from the summed correction. MACHENHAUER proposed the following solution to the problem, by assuming that after the initialization, $\ln(p_s)$ should be set to the equilibrum value obtained by filtering out the original gravity oscillations.
From (3.4) and (3.6) we get

$$\frac{\partial \ln(p_s)}{\partial t} = \underline{\pi B}^{-1} (2 \frac{\partial \eta}{\partial t}| - Q_{|\eta}) + Q_{ps} \tag{5.3}$$

assuming that the non-linear terms are constant, we integrate (5.3) :

$$\ln(p_s) = 2 \underline{\pi B}^{-1} \eta_| + (- \underline{\pi B}^{-1} Q_{|\eta} + Q_{ps}) t + \text{const} \tag{5.4}$$

By the quasi-linear approximation, $\ln(p_s)$ is composed of the η-field and a slowly varying non-linear part. The equilibrum state for η is obtained by removing the gravity waves by the initial correction $\Delta\eta$,thus at t=0 we have :

$$\ln(p_s) + \Delta \ln(p_s) = 2 \underline{\pi B}^{-1} (\eta_| + \Delta \eta_|) + \text{const}$$

hence: $$\underline{\Delta \ln(p_s) = 2 \underline{\pi B}^{-1} \Delta \eta_|} \tag{5.5}$$

As $\underline{\underline{G}}$ represents a vertical integration of the hydrostatic equation, the inverse discrete operator $\underline{\underline{G}}^{-1}$ responds with a 2-grid wave in the temperature. However, by the linear approach, the temperature correction is consistent with the temperature equation. Let $\underline{c} = \underline{\underline{\pi B}}^{-1}$, from (5.5) and from

$$\Delta\Phi_{|} = 2\Delta\eta_{|} - \overline{T}_{|}\Delta\ln(p_s) \quad \text{we arrive to}$$

$$\Delta\Phi_{|} = 2\{\underline{\underline{E}} - \overline{T}_{|}\underline{c}\}\Delta\eta_{|} \tag{5.6}$$

Here $\underline{\underline{E}}$ is the unit matrix. Correspondingly, the temperature correction is obtained

$$\Delta T_{|} = 2\underline{\underline{G}}^{-1}\{\underline{\underline{E}} - \overline{T}_{|}\underline{c}\}\Delta\eta_{|} \tag{5.7}$$

Using the definition of the $\underline{\underline{B}}$ matrix (3.6), we formally write:

$$\underline{\underline{G}}\tau = \{\underline{\underline{E}} - \overline{T}_{|}\underline{c}\}\underline{\underline{B}} \qquad \text{, hence}$$

$$\underline{\underline{G}}^{-1} = \underline{\underline{\tau B}}^{-1}\{\underline{\underline{E}} - \overline{T}_{|}\underline{c}\}^{-1} \tag{5.8}$$

and inserting in (5.7), we get

$$\underline{\Delta T_{|} = 2\underline{\underline{\tau B}}^{-1}\Delta\eta_{|}} \tag{5.9}$$

So we may think of the correction as a tendency due to the "divergence" ; $-2\underline{\underline{B}}^{-1}\Delta\eta_{|}$. As the contribution is vertically integrated by $\underline{\underline{\tau}}$, a 2-grid wave in the temperature correction is unlikely. Equation (5.9)is numerically advantageous over (5.7), as it only includes one matrix inversion.

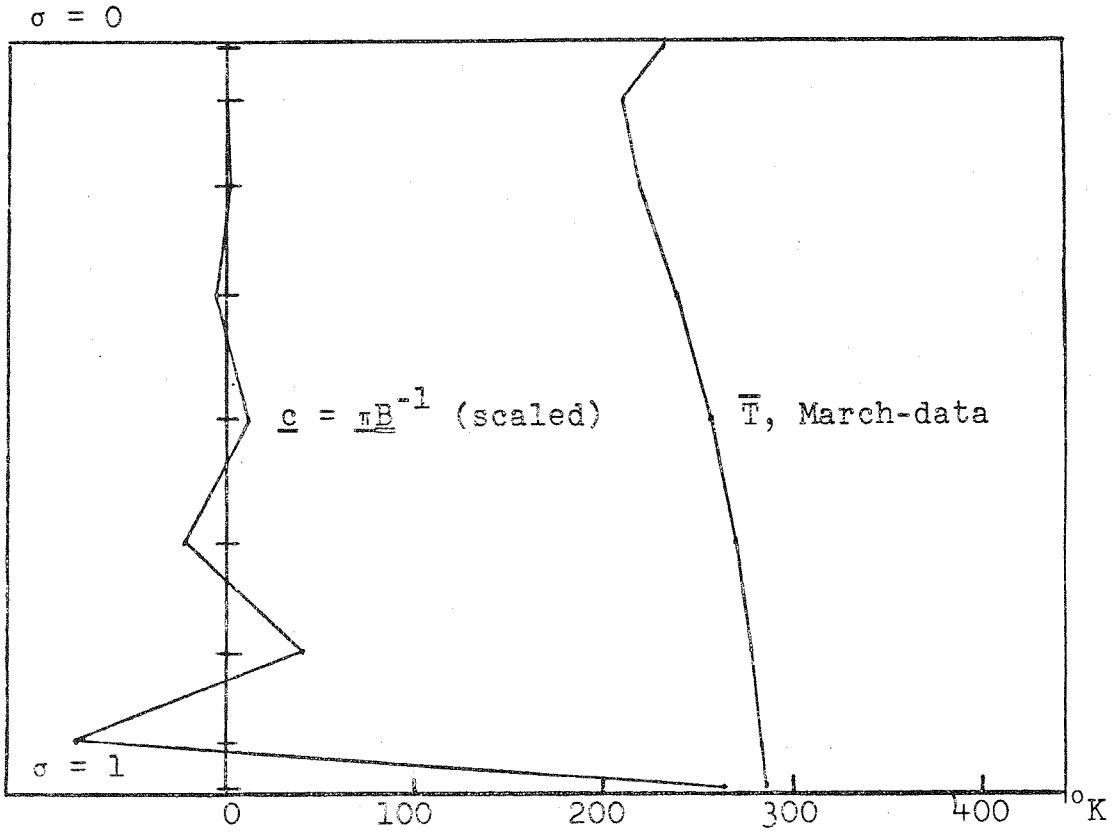

Fig.2

We may formally express the matrix inversion:

$$\{\underline{\underline{E}} - \bar{T}_{|}\underline{c}\}^{-1} = \underline{\underline{E}} + \frac{\bar{T}_{|}\underline{c}}{1 - \underline{c}\bar{T}_{|}} \qquad (5.10)$$

In the actual computations, it was observed that the product; $\underline{c}\bar{T}_{|}$ was very close to one, e.g. 0.999995 . Thus the denominator is a source of singularity in the factorization of $\underline{\underline{G}}$ in (5.8). Multiplying (5.6) by $\underline{c}$, and using (5.5), we get

$$\underline{c}\Delta\Phi_{|} = (1 - \underline{c}\bar{T}_{|})\Delta\ln(p_s) \approx (\text{small}) \qquad (5.11)$$

The plot of $\underline{c}$ (Fig.2) indicates that the geopotential correction is confined to the upper levels, by the condition of a small product; $\underline{c}\Delta\Phi_{|}$. This is consistent with the continuous picture, where the ground level is fixed by the topography.

6. Variance.

The need for control of large computations calls for an implementation of a variance, which can be checked in several stages of the transformation proces. A total field variance for a vertical mode ℓ is defined by:

$$VAR_\ell = \sum_{\substack{m=-M \\ m,n \neq 0,0}}^{M} \sum_{n=|m|}^{M} \hat{\eta}_{mn\ell} \hat{\eta}^*_{mn\ell} + \frac{H_\ell}{4}\left(\frac{\hat{\delta}_{mn\ell} \hat{\delta}^*_{mn\ell}}{n(n+1)} + \frac{\hat{\xi}_{mn\ell} \hat{\xi}^*_{mn\ell}}{n(n+1)}\right) \qquad (6.1)$$

By the requirement of a realistic vertical variance spectrum, the vertical modes are integral-normalized. However one must have in mind the lack of orthogonality of the modes.

$$\sum_{k=1}^{NL} W^2_{k\ell} \Delta\sigma_k = 1 \quad , \text{ for } \ell = 1,\ldots,NL \qquad (6.2)$$

The summed variance over the vertical modes doesnot compare to the energy of the linearized model. This is mainly due to the equivalent depth factor on the kinetic term, which makes transformation of (6.1) to single level contributions impossible even in case of orthogonality of the vertical modes. When the summed variance is computed from levels in a checking loop, it turns out that for the kinetic term, as much variance comes from coupled levels as from single levels. By orthogonality of the horizontal "Hough transformation", the variance is tactically separated into gravity-G ,and Rossby-R contributions:

$$VAR_\ell = \sum_{m=-M}^{M} \left(\sum_{k \in G_m} y_{mk\ell} y^*_{mk\ell} + \sum_{k \in R_m} y_{mk\ell} y^*_{mk\ell} \right) \qquad (6.3)$$

In a similar way, variances for the tendency fields are ob-

tained. These are measures of some balance of the atmospheric state:

$$BAL_\ell = \sum_{m=-M}^{M} \left(\sum_{k \epsilon G_m} \dot{y}_{mk\ell} \dot{y}^*_{mk\ell} + \sum_{k \epsilon R_m} \dot{y}_{mk\ell} \dot{y}^*_{mk\ell} \right) \qquad (6.4)$$

As the contributions in (6.3) and (6.4) are divided for flow parity, we arrive to a multiple of 8 parameters for each vertical mode. These parameters are printed out for monitoring of the iteration step.

	symmetric	antisym.
gravity	SGVAR	AGVAR
	SGBAL	AGBAL
Rossby	SRVAR	ARVAR
	SRBAL	ARBAL

7. Results

The initialization experiment was performed with the 9-level ECMWF spectral model at a triangular truncation 21 (hereinafter referred to as T21). The reader is referred to an internal report of A.W.HANSEN and A.BAEDE for further details of T21. Initial data refers to the situation on 1´st of march 1965. In Fig.3 the rate of convergence is displayed from an initialization with correction of 5 vertical modes, the curves are numbered according to the iteration step. After only one iteration, the GBAL is below the initial balance of the Rossby waves, and in the final step, the overall GBAL is reduced by a factor of about 4×10^{-5}. It was a main objective of this work to clarify whether the non-linear initialization was convergent when applied to a model with physical processes included. In Fig.4

the results are shown from the non-adiabatic T21 model, which includes the GFDL physical parameterization package. Again the convergence is fair, but for the higher modes: H_6-H_8, the initial GBAL increases compared to the adiabatic version, the curve is slightly pulled down in the iteration step due to lack of complete orthogonality. These modes, having their larger amplitude at low level, are affected by boundary layer processes. The mode: H_7 where a kink on the curve appears, has a great amplitude at the first level. An attempt to activate the modes H_0-H_6 in the iteration procedure, led to an explosive growth of GBAL for the higher modes H_5-H_8. This indicates that the convergence is mainly established from the adiabatic part of the tendencies. The effect of initialization to the 500 mb and 850 mb height fields are shown in fig.(5-11). The maps look very much unaffected; however, the Atlantic depression 45°W, 50°N are deepened by about 70m for the 500 mb map. Near the Pacific low 170°W, 45°N the gradients are amplified, increasing the geostrophic winds. The initialization is by no means a space smoothing operation.

The divergence fields (see fig. 12-20) are substantially reduced by the initialization so that very little connection with the original fields is left. By this, the strange elongated patterns across the maps disappear.

Differences between adiabatic and non-adiabatic computations are expected near the surface. By the vertical resolution used, this is reflected in the 850 mb maps. An increased convergence in the Atlantic low is seen, this apparently is connected with the included friction terms.

A 10 day integration from the nonlinear-nonadiabatic initialized dataset was performed by A. BAEDE. The pressure oscillations clearly disappear (see fig. 21), however, by the inclusion of a weak time filter, the model is able to dampen the oscillations in about 4 days, but in general the integrations do not converge. From the global RMS difference of the height fields it is interestingly seen that a slight minimum appears on about day 3, and from hereon it increases regularly.

Regarding the pattern of precipitation, accumulated over 12 and 24 hours, no substantial differences due to initialization have been found.

8. Conclusions

A full multi-level initialization program has been put together, in order to take advantage of the non-linear initialization method. However, the program is not in an optimal state for the CDC 6600 computer. Efforts are made to reduce the storage of fields in core, so that the initialization can be performed from one program only. As a by-product, normal mode statistics can be found from data series, e.g. KASAHARA (1976). The multi-level program has in general the same efficiency in removing the noise, as was demonstrated by MACHENHAUER (1977) in a baro-tropic spectral model.

APPENDIX. Storage of eigenvectors and eigenvalues

For each vertical mode, a binary record is built by storing the eigenvectors column-wise, the record length will be

$$\sum_{m=0}^{M} N_{OR}^2(m)$$

where N_{OR} is the matrix order (p.11). Likewise,the eigenvalue record length is

$$\sum_{m=0}^{M} N_{OR}(m)$$

For convenience, the same storage picture is used for both symmetric and antisymmetric case, i.e. N_{OR} is symmetrical determined. The total requirements of words on the disk is therefore the sum of these lengths multiplied by 2 , and by the number of vertical modes; NL. By use of some algebra, this amounts to

$$\text{words} = \begin{cases} \frac{3}{2}(M+1)(M+2)(M+3)NL & M \text{ odd} \\ \frac{3}{2}M(M+1)(M+2)NL + & \\ 2\left(\left(\frac{3}{2}M+2\right)^2 + \frac{3}{2}M+2\right)NL & M \text{ even} \end{cases}$$

NL=9

M	21	40	60	80
words	163944	1000188	3217428	7443468

If only the modes active for the iteration step are considered, storage requirements can be cut down to about one third of these estimates.

Acknowledgements

I am grateful to Mr. A.W.Hansen for his advice and for providing the spectral model to my disposal, to Dr. B.Machenhauer who has suggested this work, and to Mr. C.Temperton for reading the manuscript.

References

Bourke,W.(1974) A Multi-Level Spectral Model. I.Formulation and Hemispheric Integrations. Monthly Weather Review,102, pp. 687-701.

Eliasen,E. and Machenhauer,B. (1969) On the observed large-scale wave motions. Tellus XXI,2, pp 149-166.

Hansen,A.W. and Baede,A. (1977) Unpublished.

Hoskins,B.J. and Simmons,A.J. (1975) A multi-layer spectral model and the semi-implicit method. Quart.J.R.Met-Soc.,101, pp. 637-655.

Kasahara,A. (1976) Normal Modes of Ultralong Waves in the Atmosphere. Monthly Weather Review,104, pp. 669-690.

Longuet-Higgins,M.S. (1968) The eigenfunctions of Laplace's tidal equations over a sphere. Phil.Trans.Roy.Soc.London A262, pp. 511-607.

Machenhauer,B. (1977) On the Dynamics of Gravity Oscillations in a Shallow Water Model, with Applications to Normal Mode Initialization. Beiträge zur Physik der Atmosphäre,50, pp. 253-271.

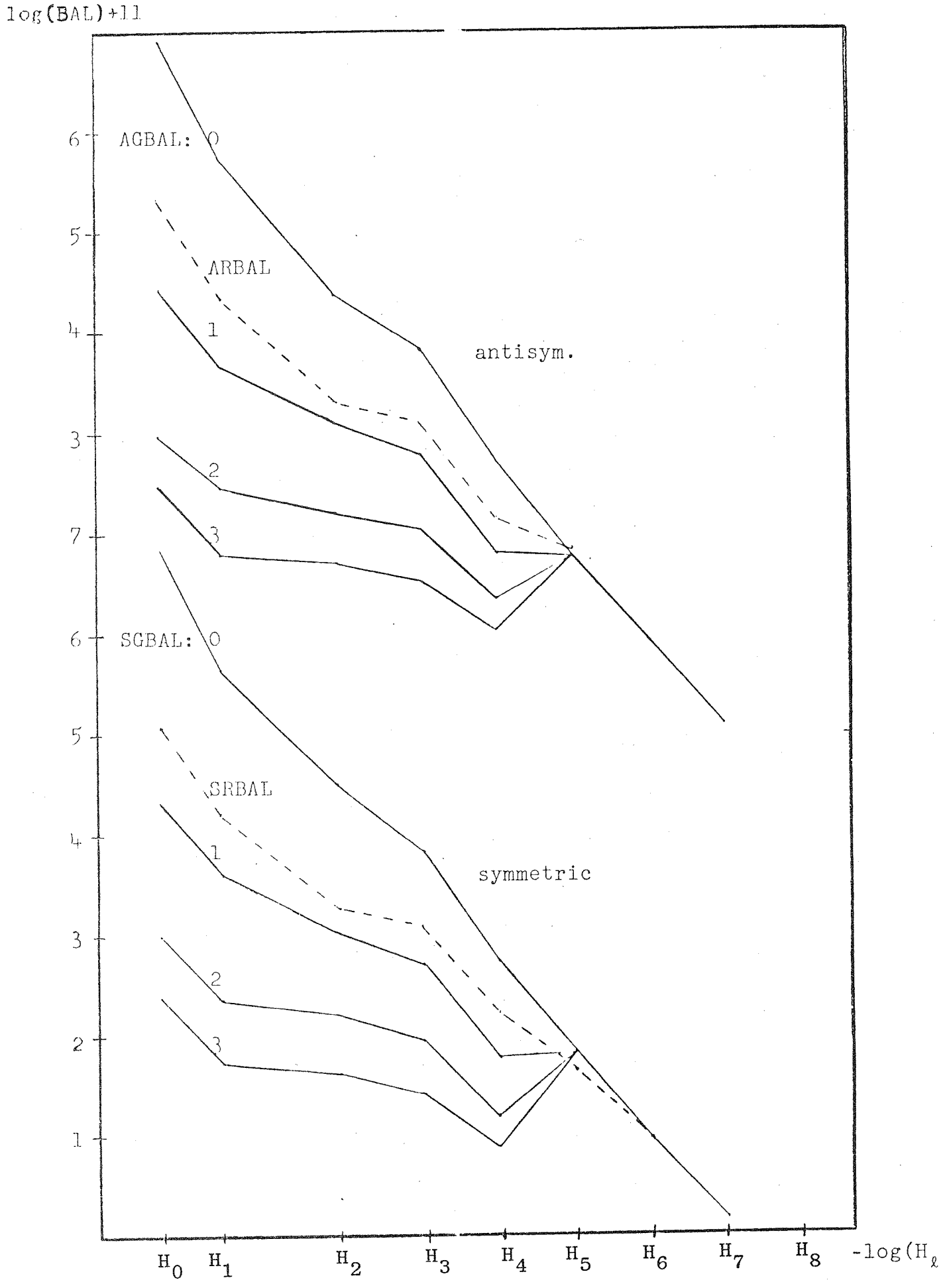

Fig.3 Adiabatic 5-modes initialization

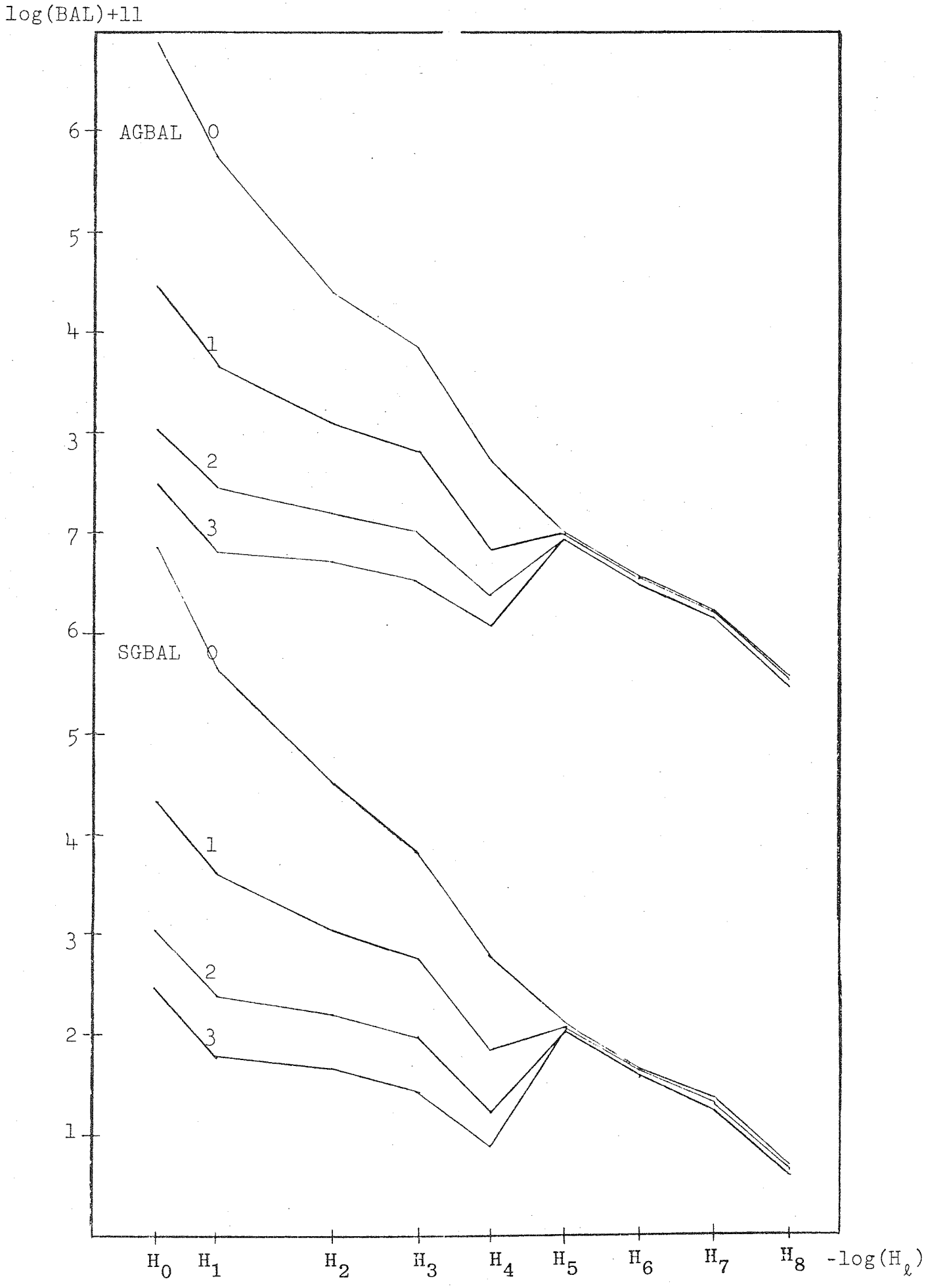

Fig.4 Non-adiabatic 5-modes initialization

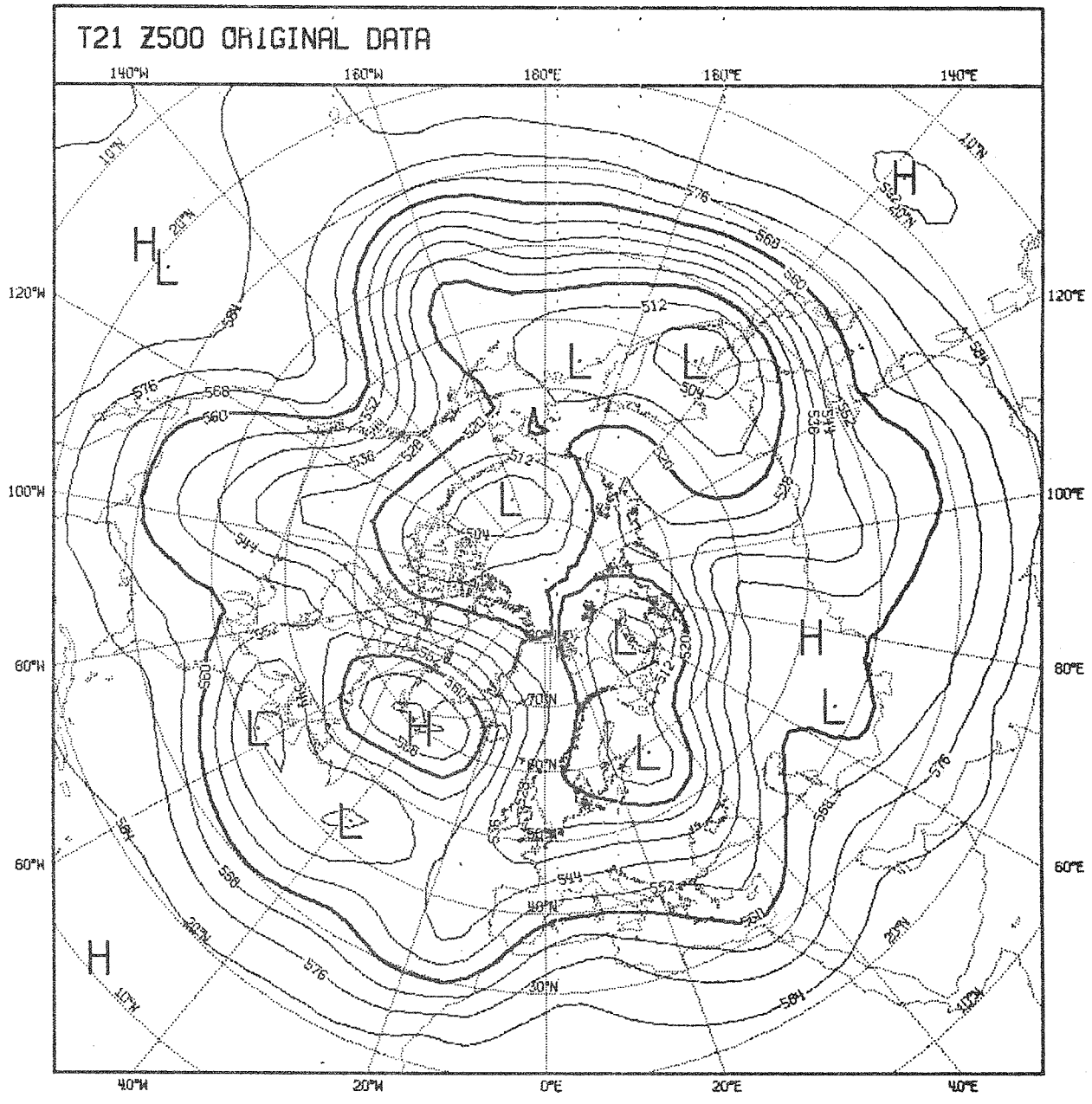

Fig.5

500 mb height field,analysed 1-3-1965 (10m.unit)

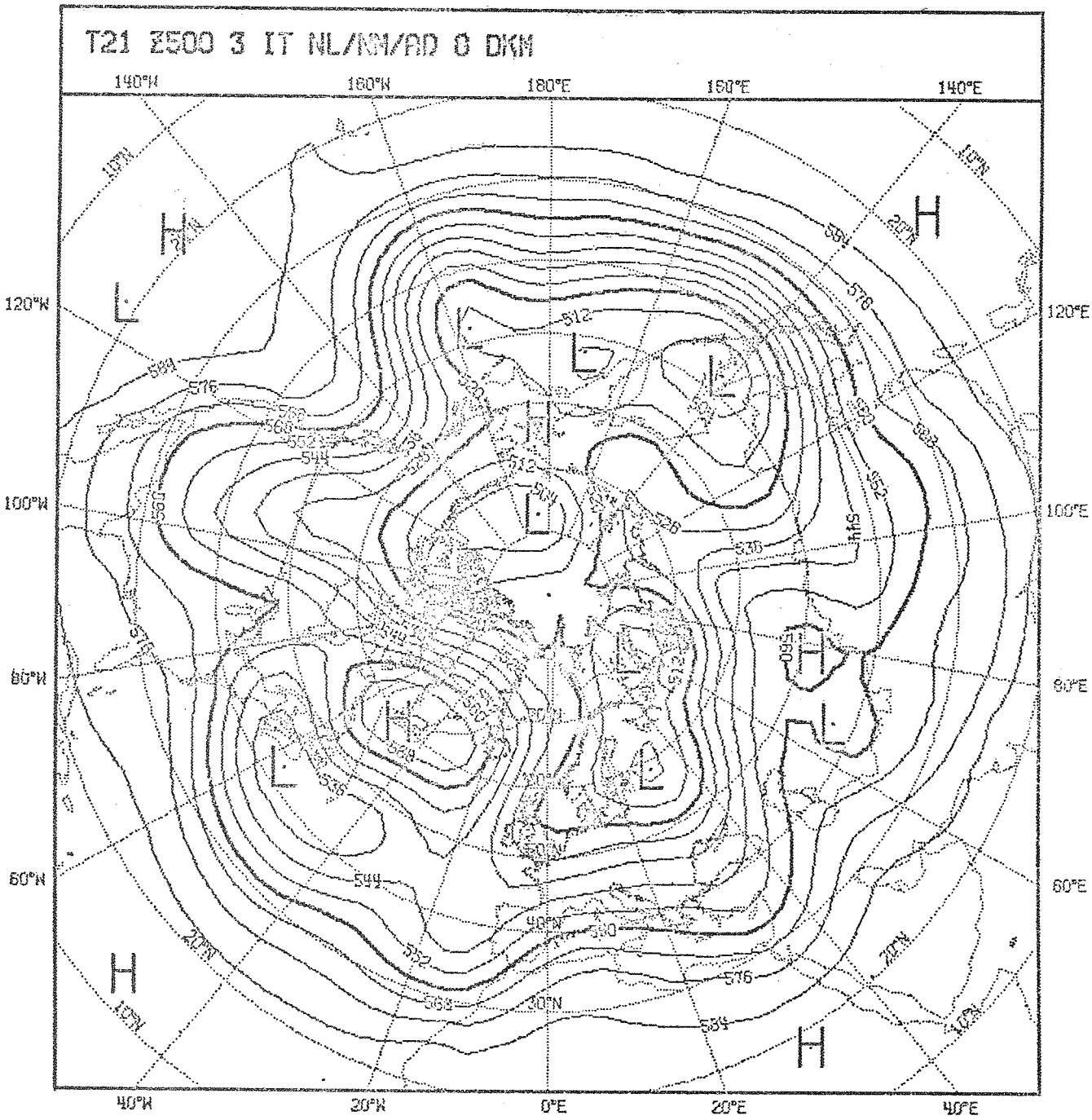

Fig.6

500 mb height field after 5 modes adiabatic initialization

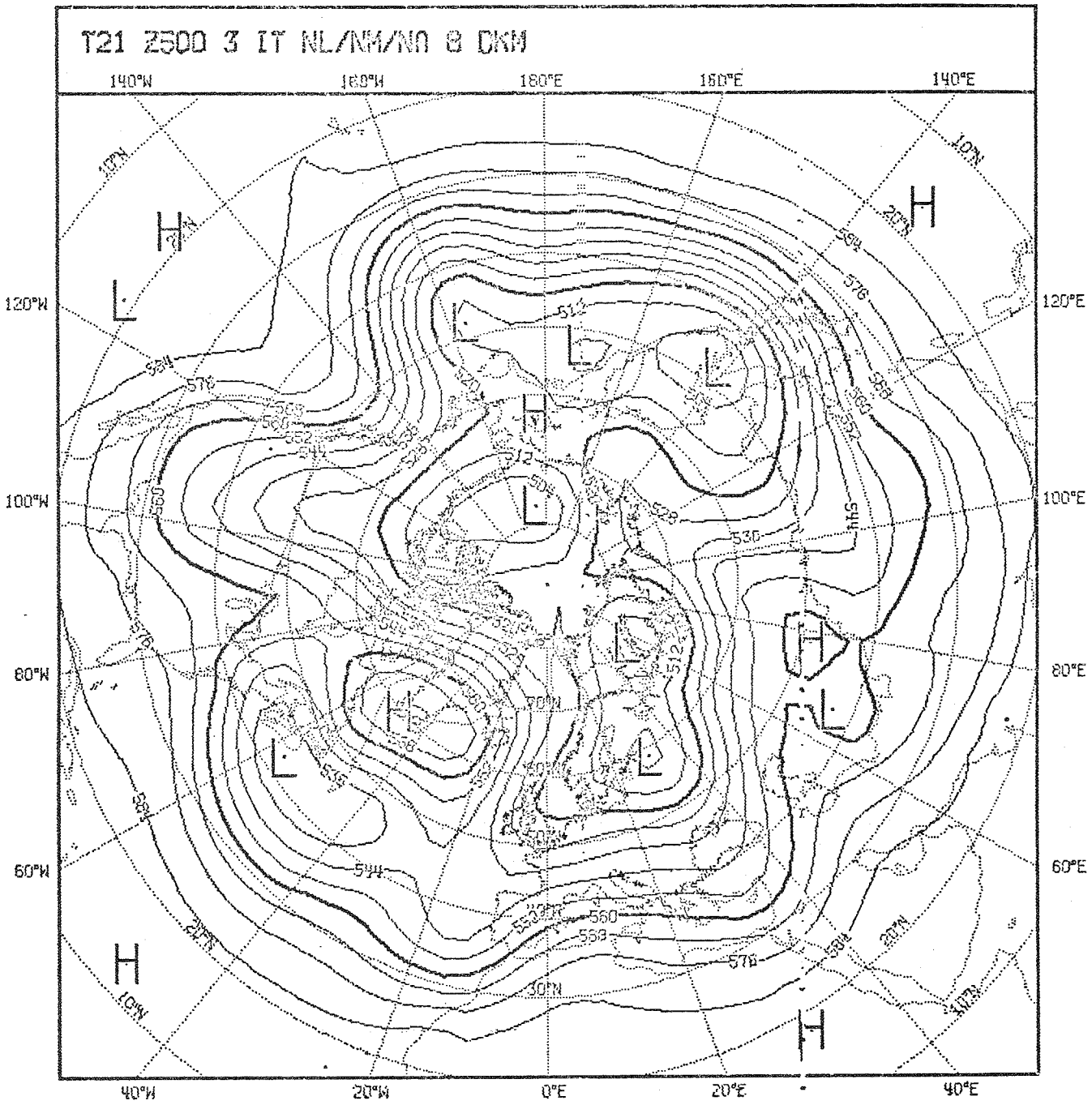

Fig.7

500 mb height field after 5 modes non-adiabatic initialization

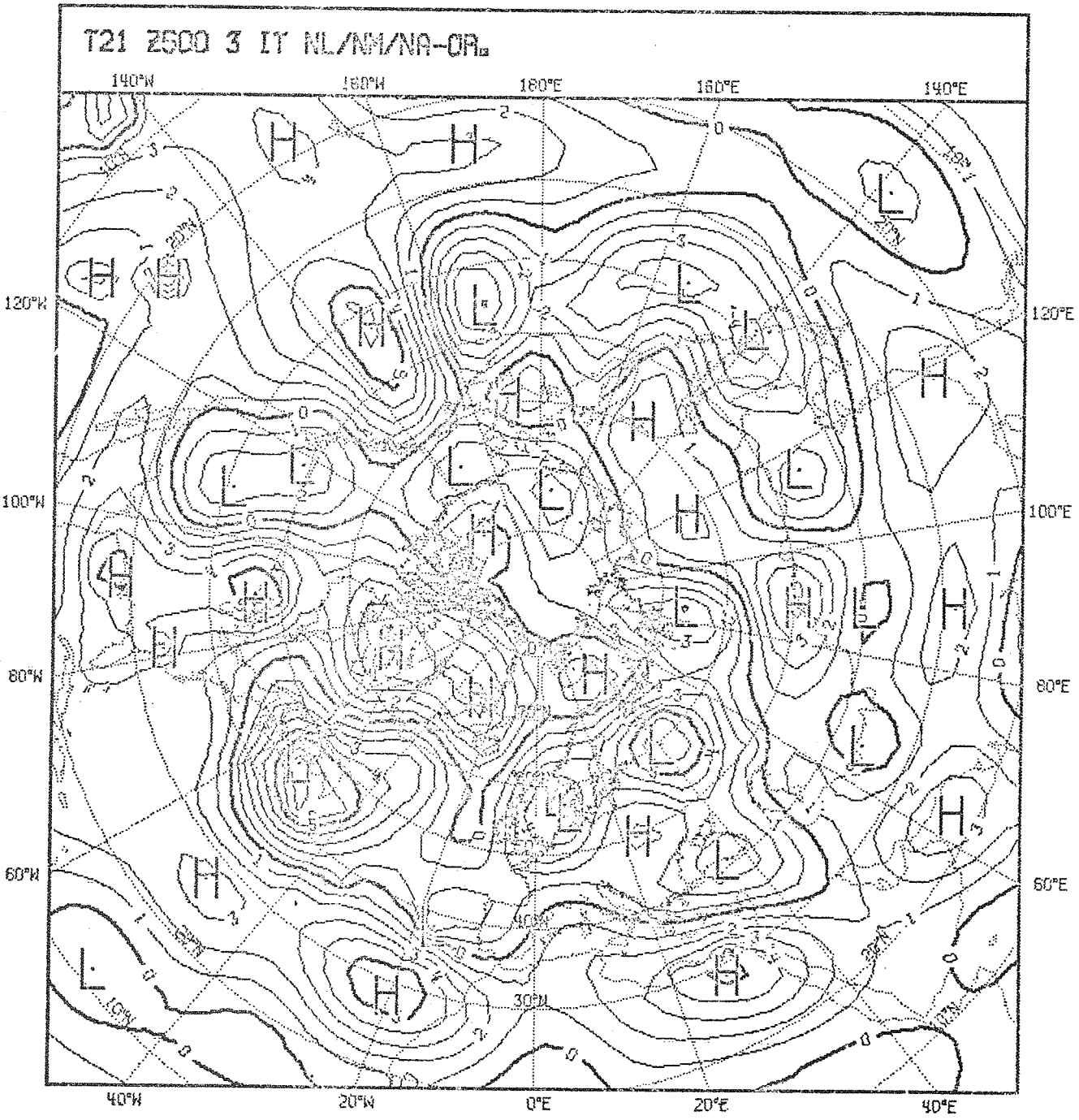

Fig.8

difference between non-adiabatic initialized and original 500 mb fields.

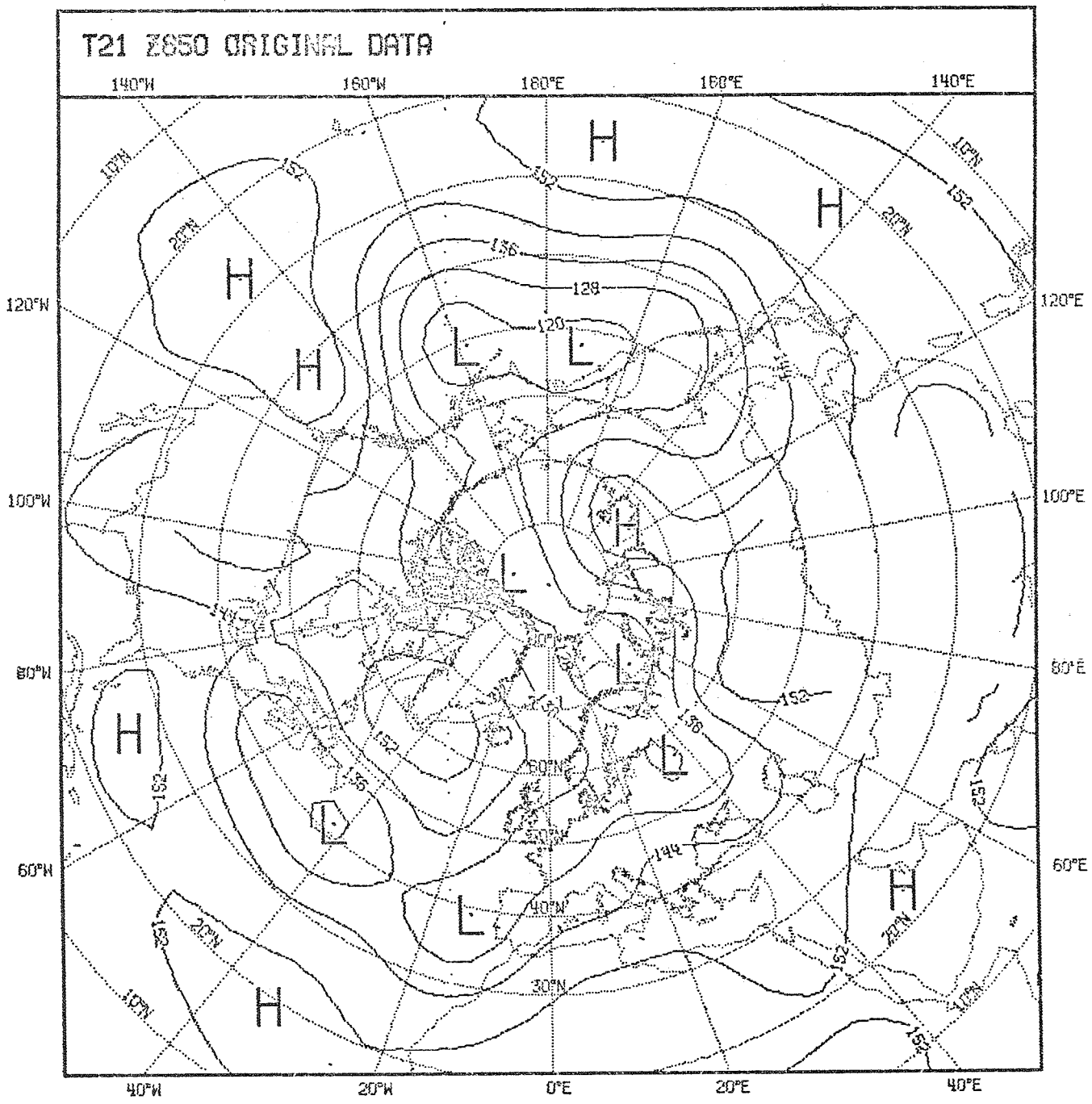

Fig.9

850 mb height field, analysed 1-3-1965 (10m.)

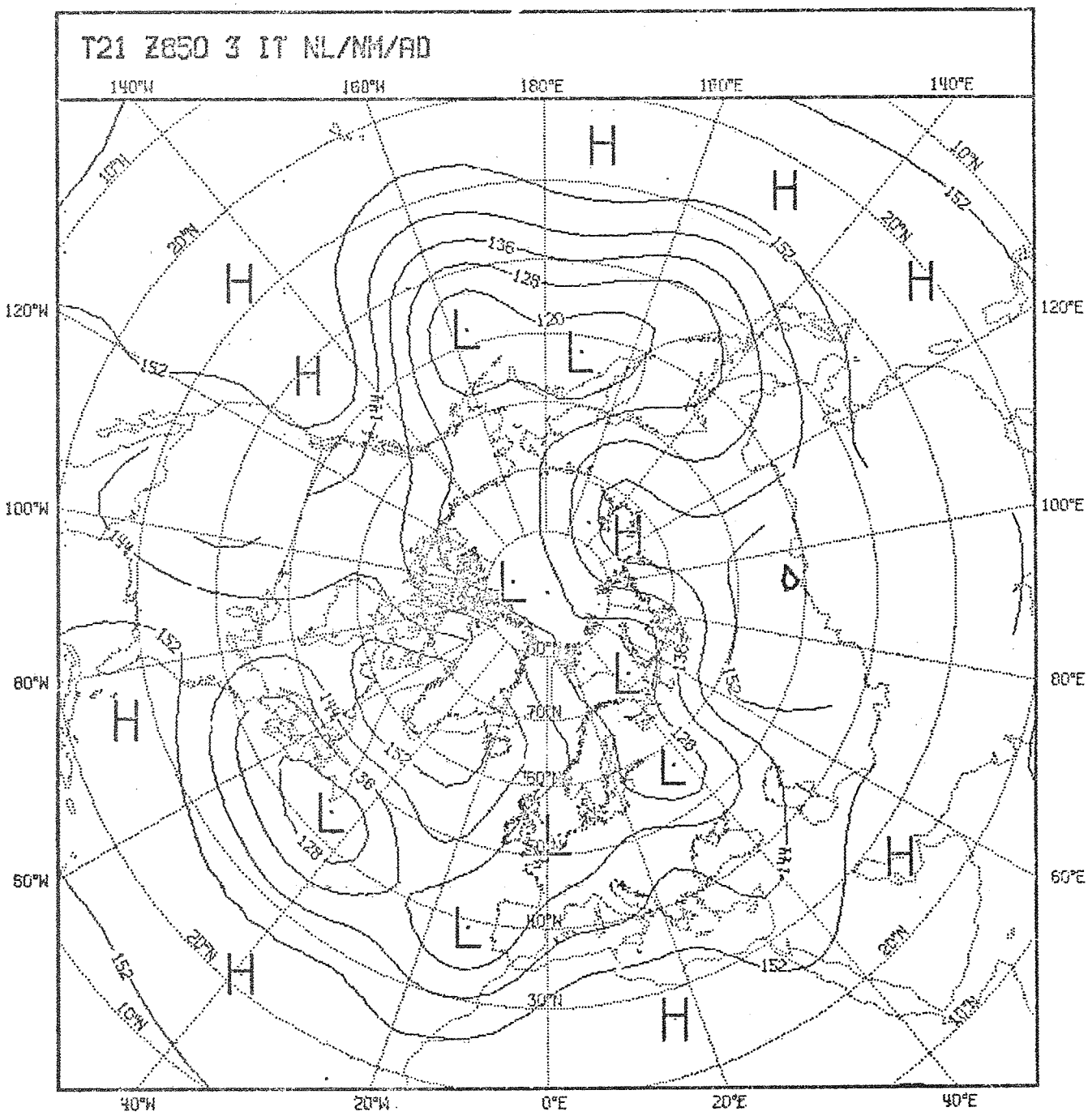

Fig.10

850 mb height field after 5 modes adiabatic initialization

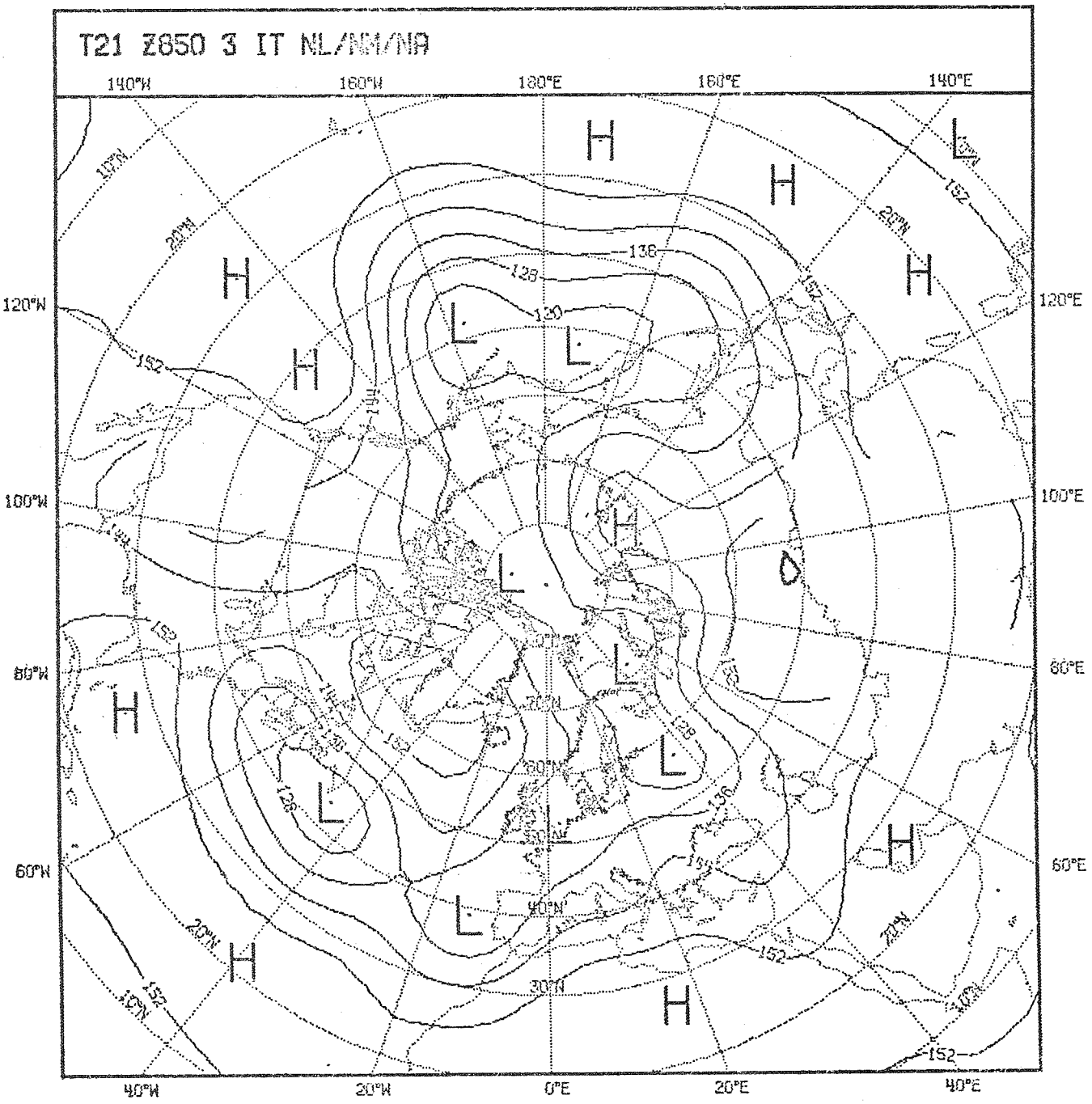

Fig.11

850 mb height field after 5 modes non-adiabatic initialization

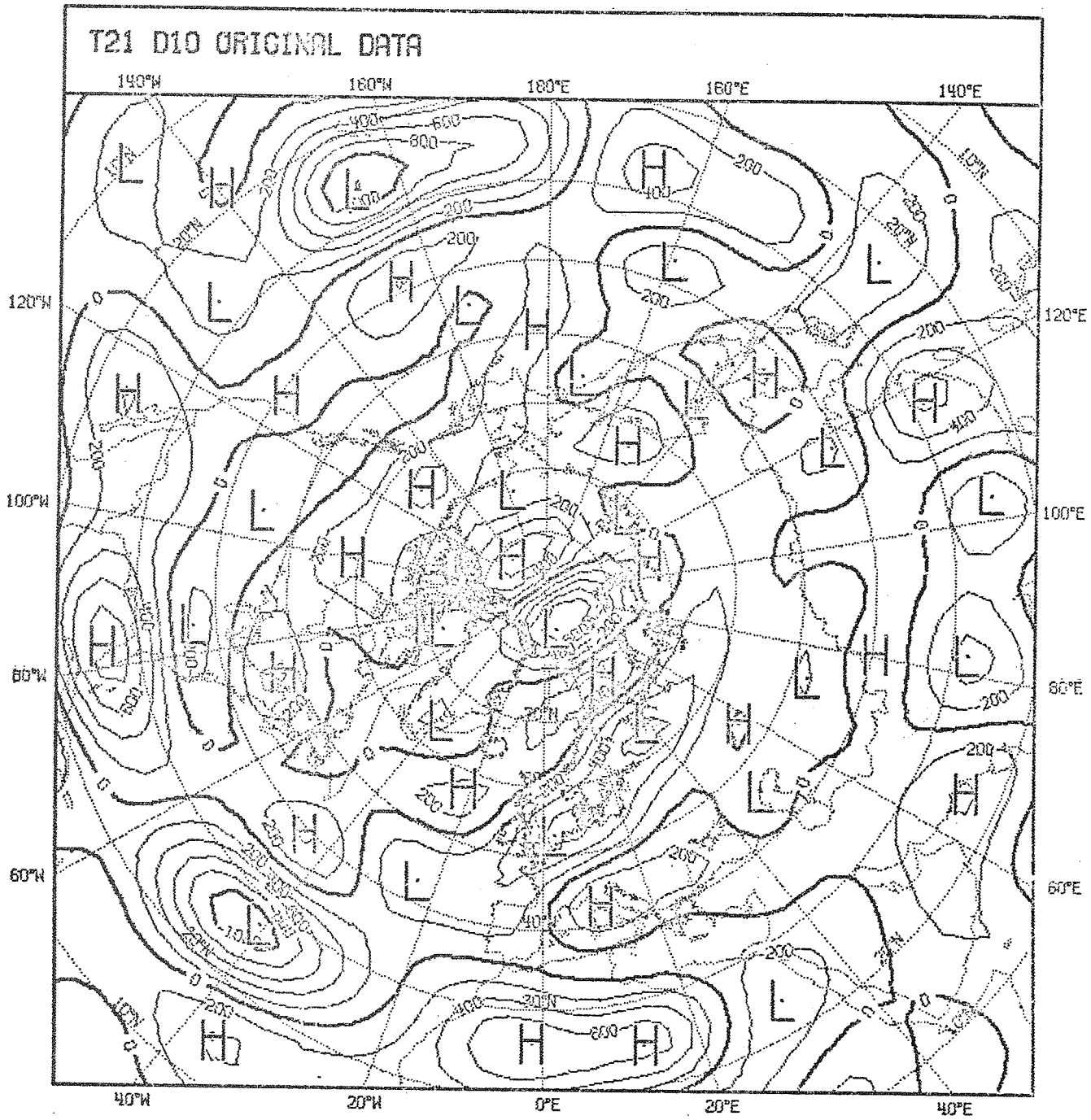

Fig.12

10 mb divergence field, analysed 1-3-1965 (10^{-8} sec^{-1})

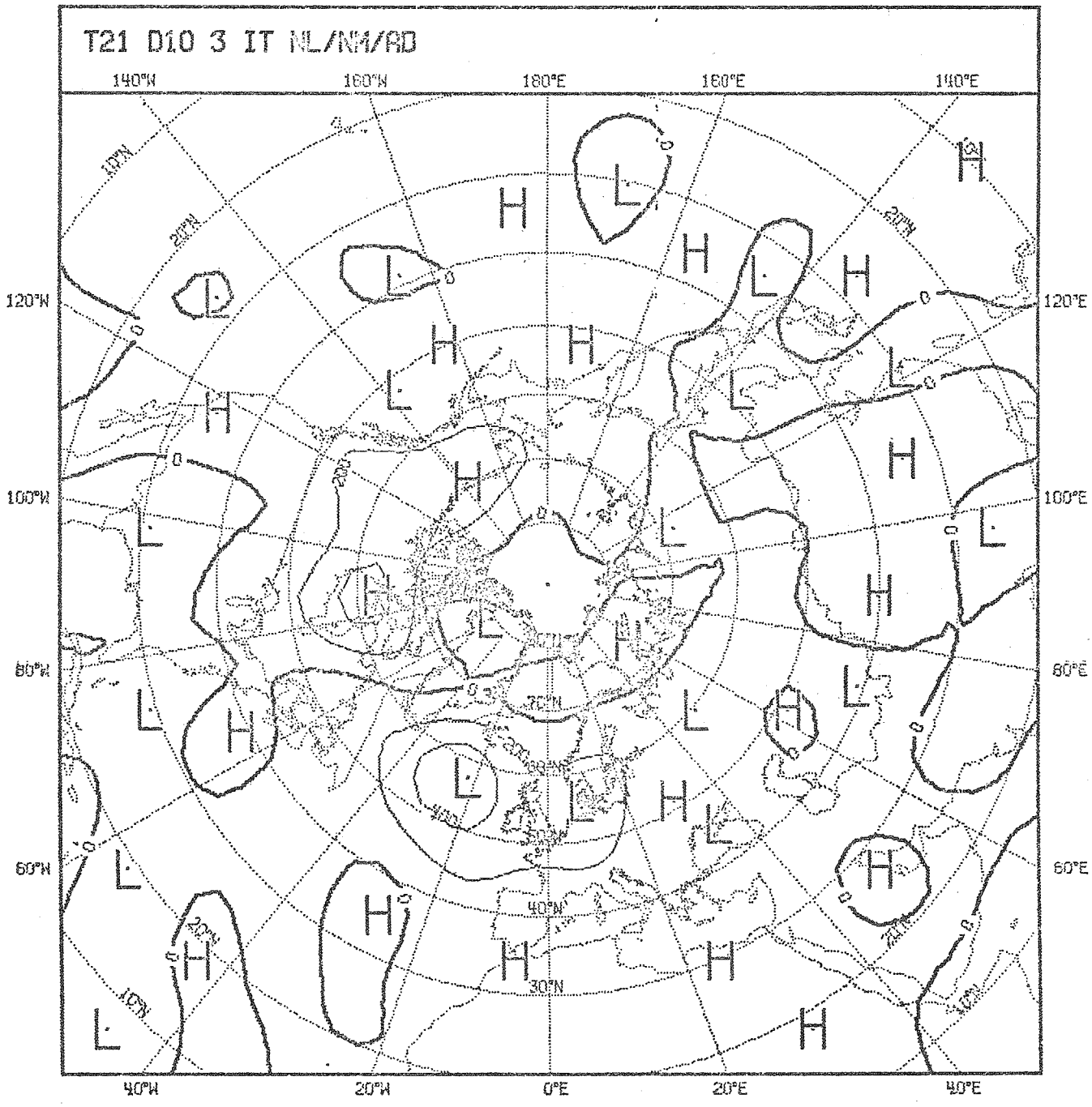

Fig.13

10 mb divergence field after 5 modes adiabatic initialization

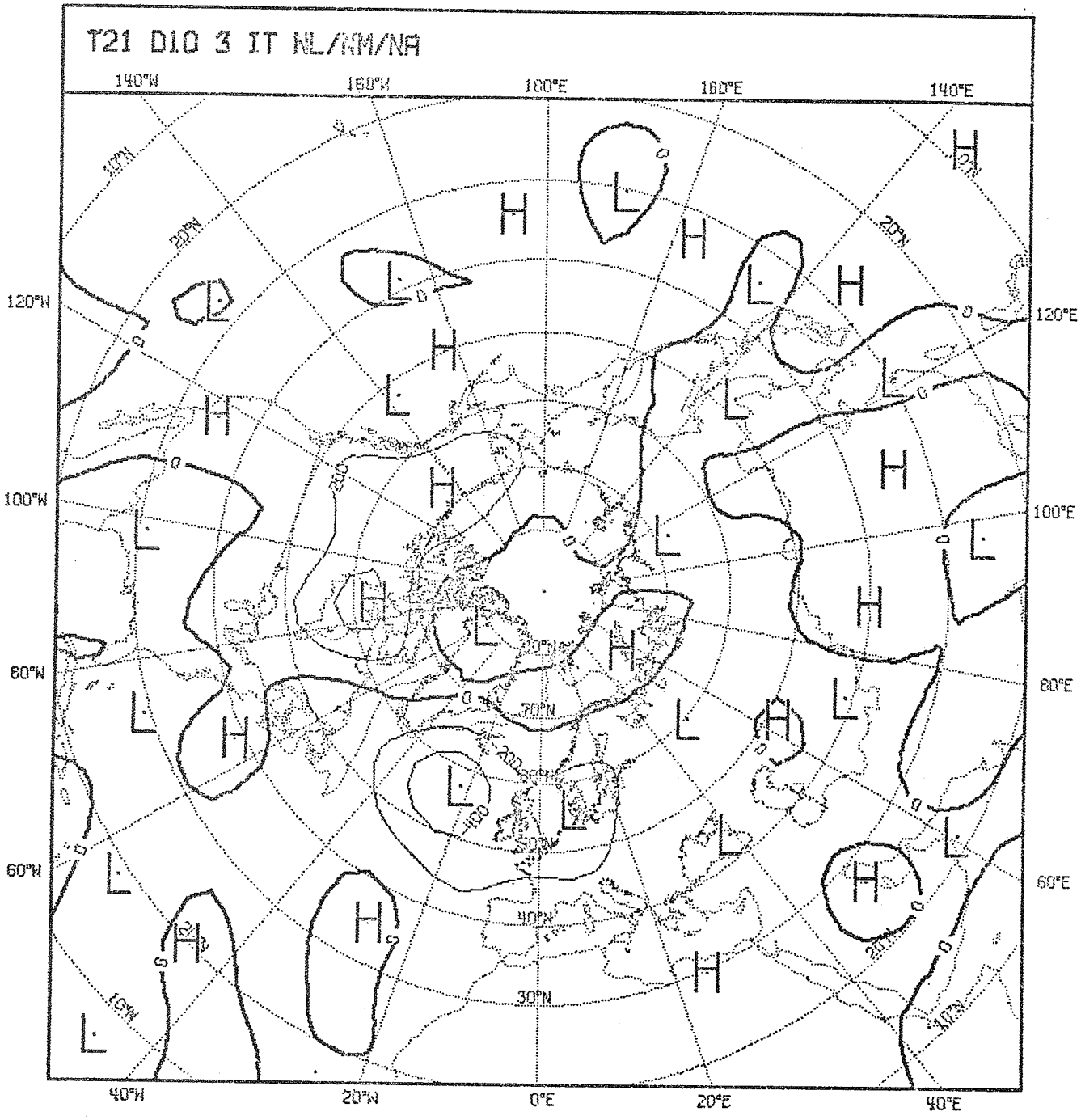

Fig.14

10 mb divergence field after 5 modes non-adiabatic initialization

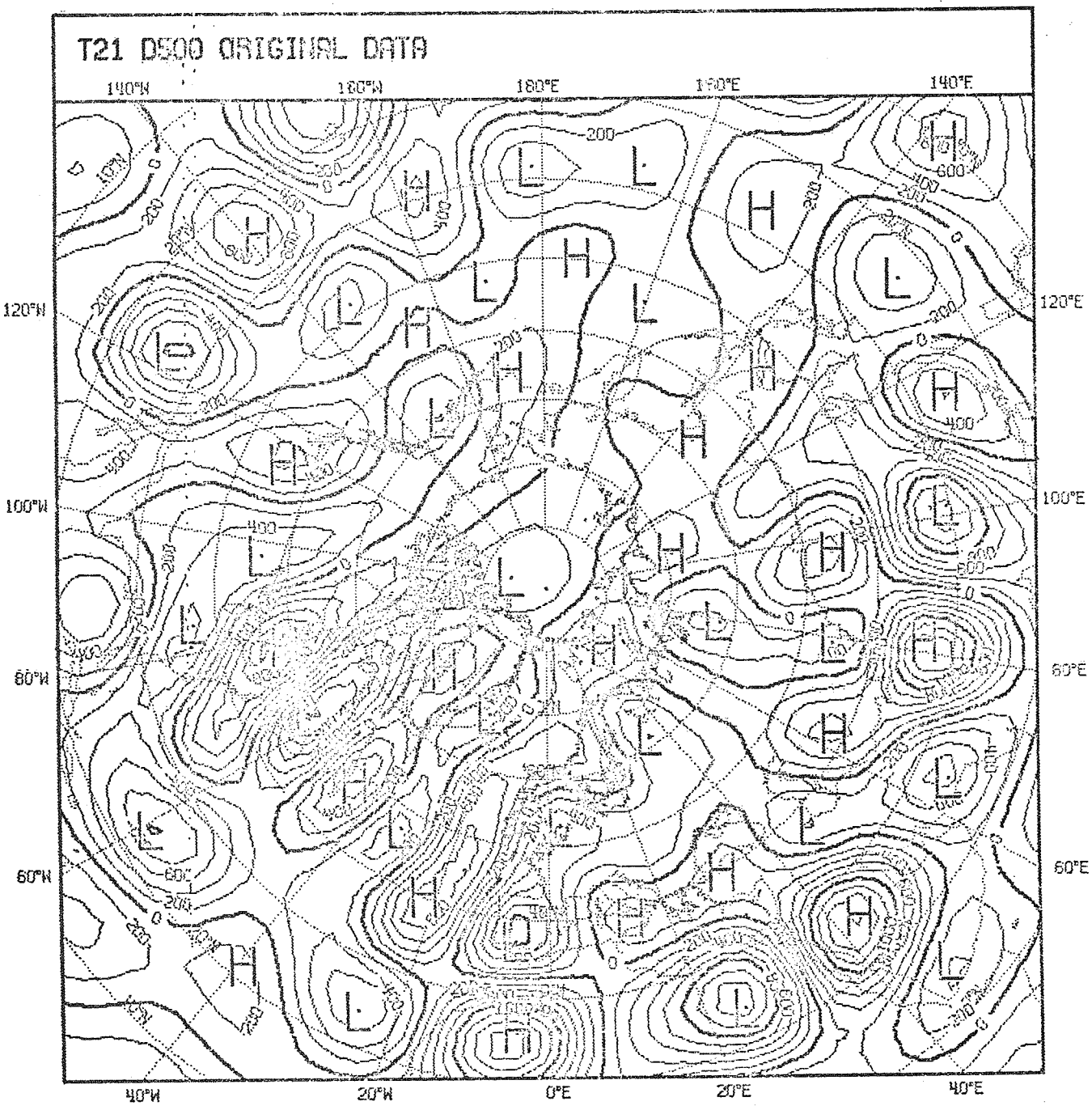

Fig.15

500 mb divergence field, analysed 1-3-1965 (10^{-8}sec^{-1})

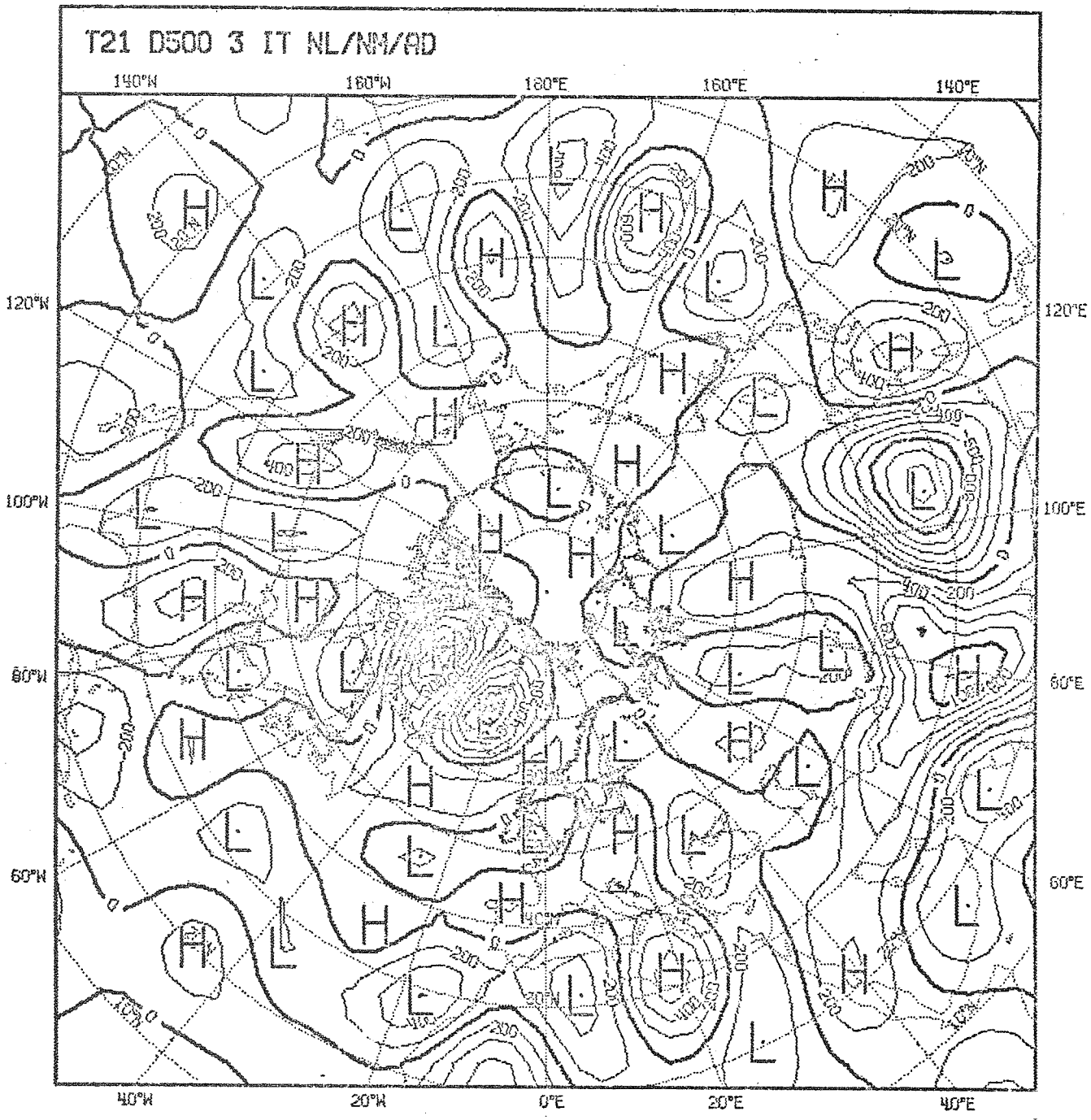

Fig.16

500 mb divergence field after 5 modes adiabatic initialization

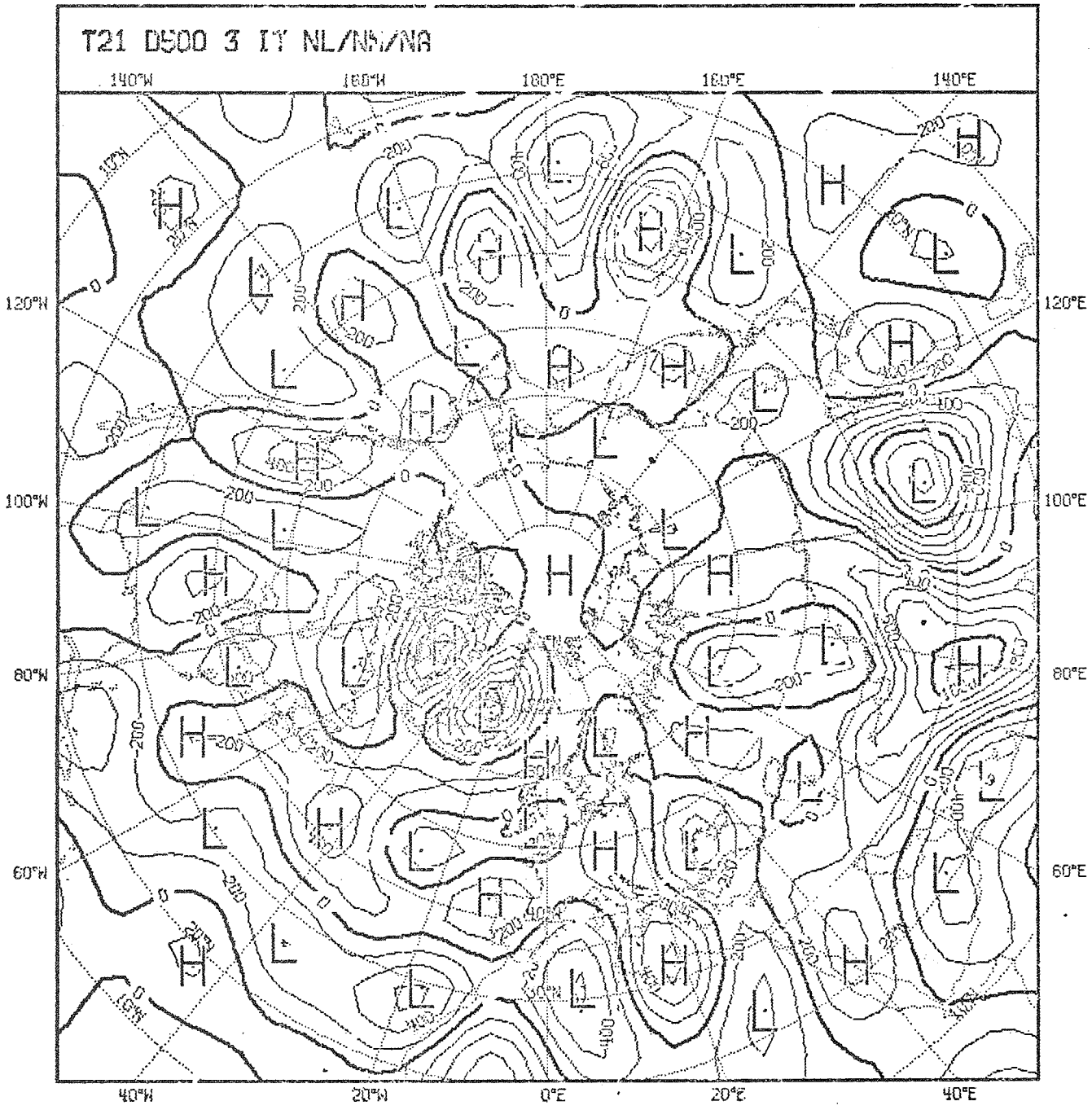

Fig.17

500 mb divergence field after 5 modes non-adiabatic initialization

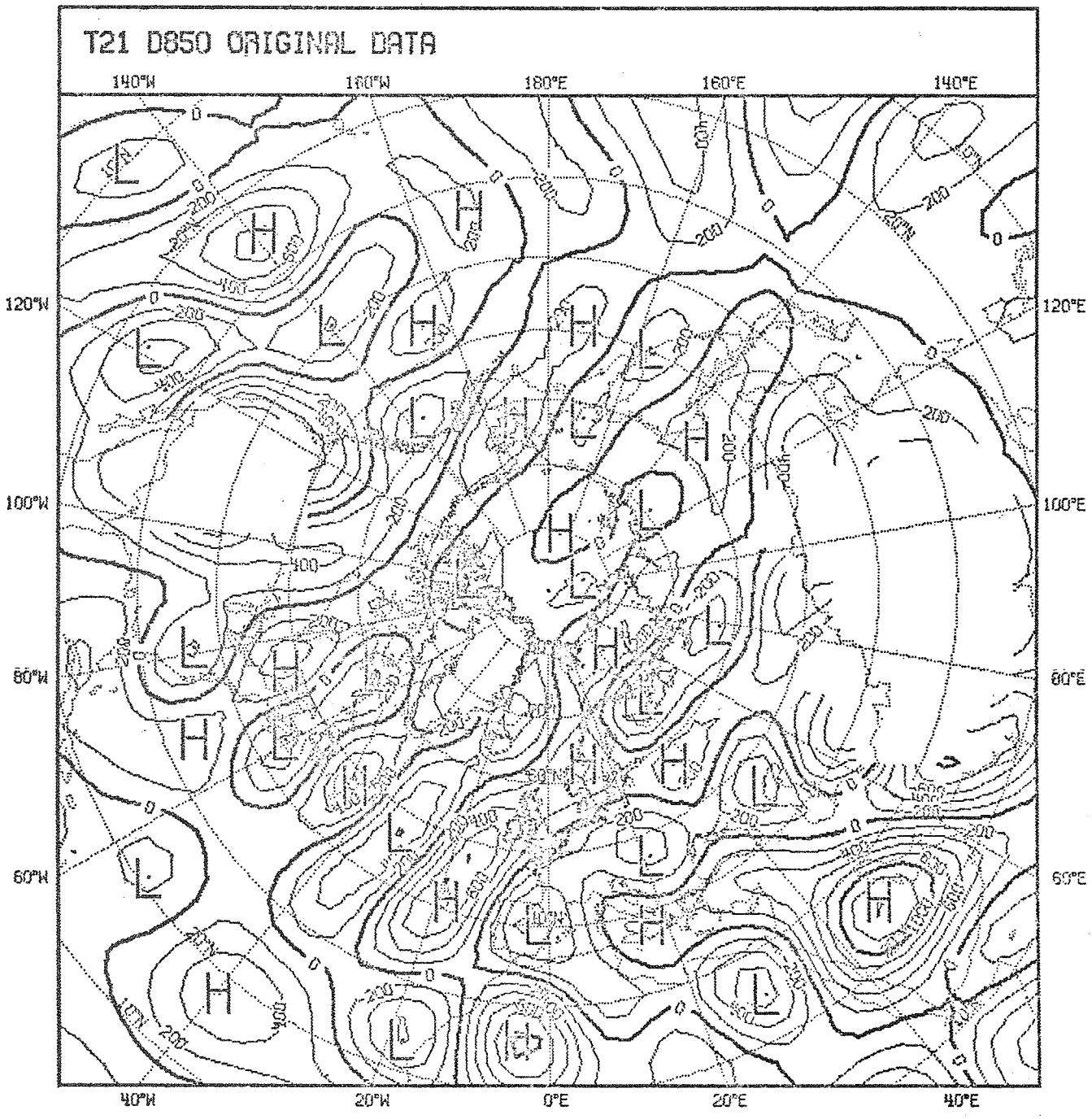

Fig.18

850 mb divergence field, analysed 1-3-1965 (10^{-8}sec^{-8})

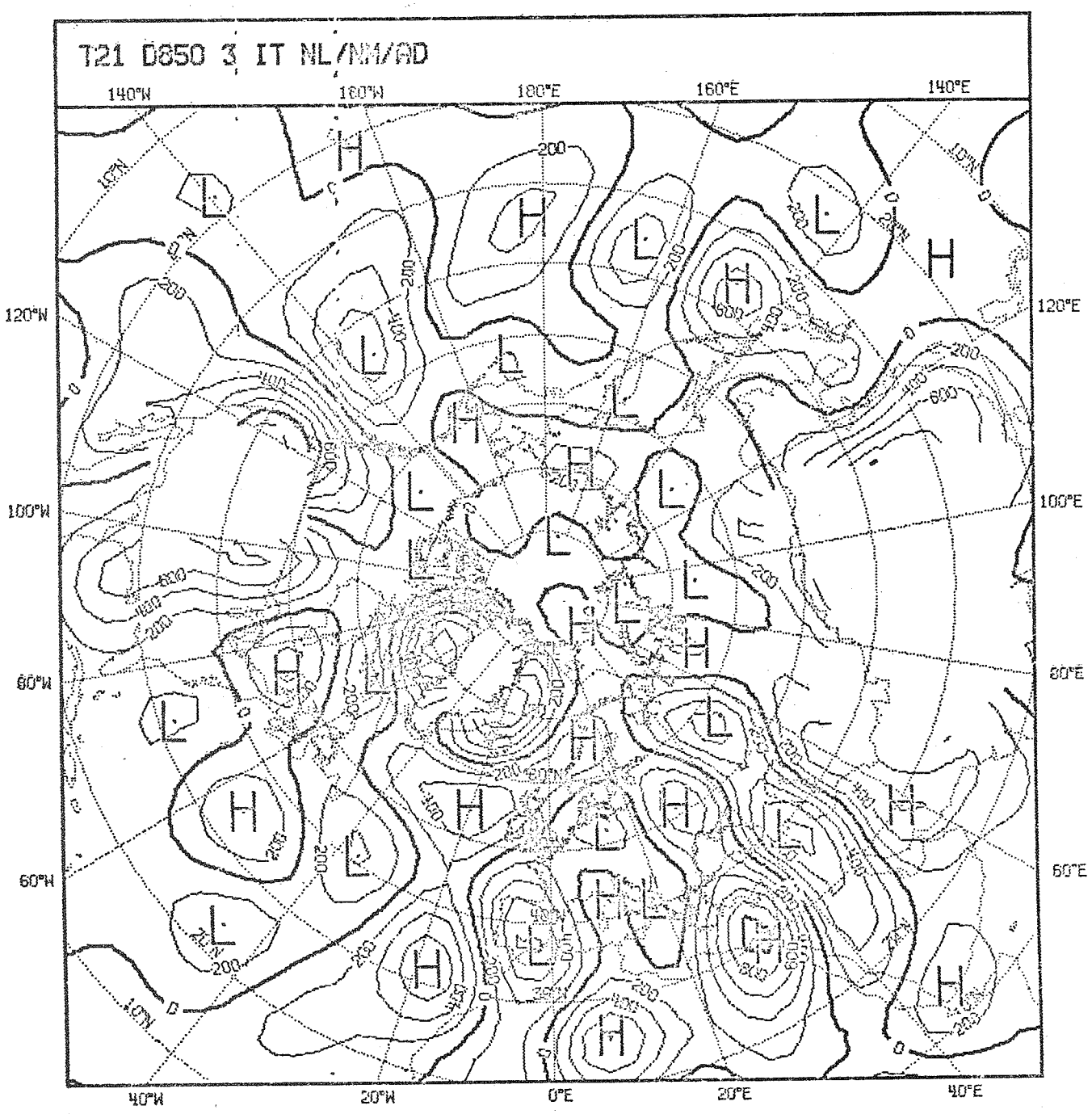

Fig.19

850 mb divergence field after 5 modes adiabatic initialization

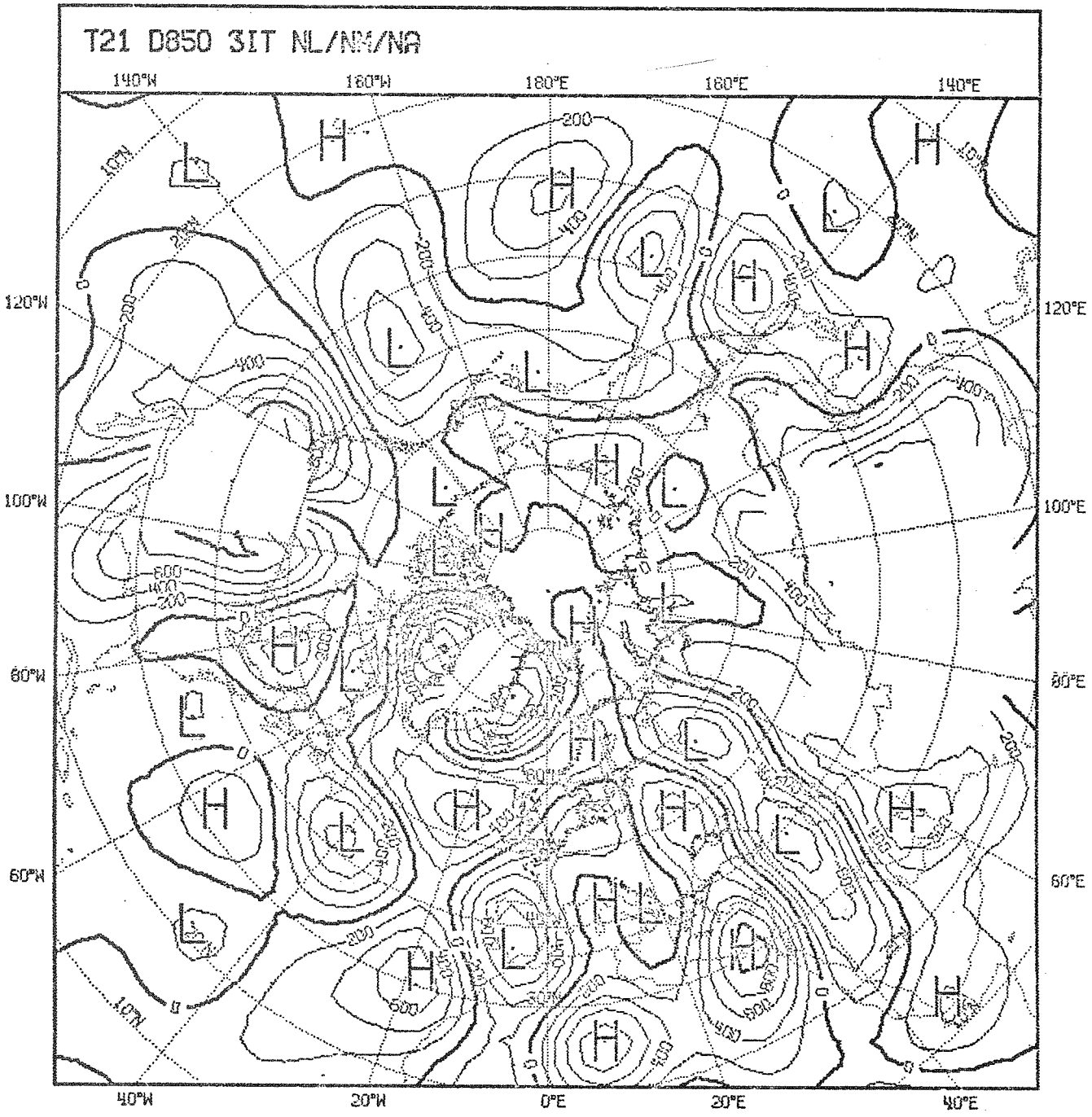

Fig.20

850 mb divergence field after 5 modes non-adiabatic initiali-ation

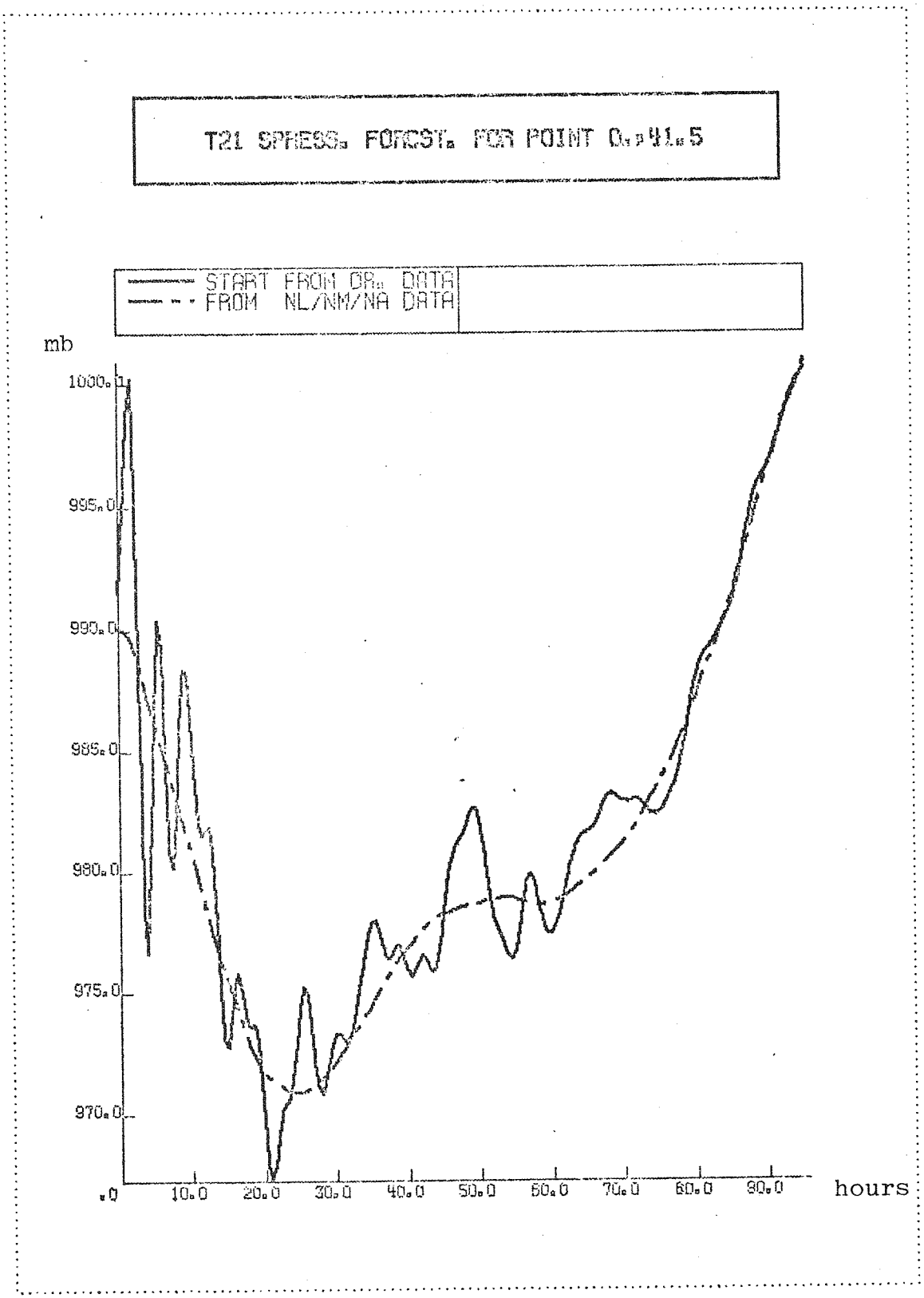

Fig.21

The effect of initialization for the surface pressure forecast of a gridpoint located at $(\lambda,\phi) = 0^{\circ}.,41^{\circ}.5$

EUROPEAN CENTRE FOR MEDIUM RANGE WEATHER FORECASTS

Research Department (RD)

Internal Report No. 15

No. 1 Users Guide for the G.F.D.L. Model
(November 1976)

No. 2 The effect of Replacing Southern Hemispheric Analyses by Climatology on Medium Range Weather Forecasts
(January 1977)

No. 3 Test of a Lateral Boundary Relaxation Scheme in a Barotropic Model
(February 1977)

No. 4 Parameterization of the Surface Fluxes
(February 1977)

No. 5 An Improved Algorithm for the Direct Solution of Poisson's Equation over Irregular Regions
(February 1977)

No. 6 Comparative Extended Range Numerical Integrations with the ECMWF Global Forecasting Model 1: The N24, Non-Adiabatic Experiment
(March 1977)

No. 7 The ECMWF Limited Area Model
(March 1977)

No. 8 A Comprehensive Radiation Scheme designed for Fast Computation
(May 1977)

No. 9 Documentation for the ECMWF Grid-Point Model
(May 1977)

No. 10 Numerical Tests of Parameterization Schemes at an Actual Case of Transformation of Arctic Air
(June 1977)

No. 11 Analysis Error Calculations for the FGGE
(June 1977)

No. 12 Normal Modes of a Barotropic Version of the ECMWF Grid-Point Model
(July 1977)

No. 13 Direct Methods for the Solution of the Discrete Poisson Equation: Some Comparisons
(July 1977)

No. 14 On the FACR(ℓ) Algorithm for the Discrete Poisson Equation
(September 1977)

No. 15 A Routine for Normal Mode Initialization with Non-Linear Correction for a Multi-Level Spectral Model with Triangular Truncation
(August 1977)